Airway Disease

Tullio Valente

Contents

1	**Acute Lower Airway Obstruction and Aspiration**	000
1.1	Introduction	000
1.2	Imaging	000
1.3	Pulmonary Parenchymal Abnormalities	000
1.4	Acute Aspiration	000
1.5	Summary	000
2	**Acute Exacerbation of Bronchiectasis**	000
2.1	Introduction	000
2.2	Acute Exacerbations	000
2.3	Clinical and Imaging Diagnosis	000
2.4	Summary	000
3	**Toxic Gas Inhalation**	000
3.1	Introduction	000
3.2	Definitions and Classification	000
3.3	Mechanisms of Toxicity	000
3.4	Clinical Setting, Imaging, and Management	000
3.5	Some Unique Pulmonary Acute Toxins and Toxicants	000
3.6	Summary	000
References		000

T. Valente
Department of Imaging, Section of Radiology,
Azienda Ospedali dei Colli,
P.O. Monaldi, Naples 80100, Italy
e-mail: tullio.valente@gmail.com

Abstract

There are few conditions in emergency medicine as potentially challenging and high risk as the *acute airway obstruction*. Time is often limited, the patient's condition may be critical, and a failed airway has the potential for significant morbidity or death. Chest radiography (CXR) is useful in diagnosing and evaluating the progression of atelectasis, aspiration, pulmonary edema, pneumonia, and pleural fluid collections. Lung ultrasonography (LUS) is an excellent complementary diagnostic tool in emergency diagnosis. For patients who can tolerate lying flat for the study, thin-section multidetector computed tomography (MDCT) provides the anatomic detail that permits planning of therapy and is useful when the clinical and radiologic presentations are discrepant and the patient is not responding to therapy or in further defining a radiographic abnormality.

Imaging plays a key role in the diagnosis and monitoring of *bronchiectasis* and the management of complications. Exacerbation of bronchiectasis can confer substantial potential morbidity, usually secondary to recurrent infection. In severe cases of bronchiectasis, massive hemoptysis can lead to death. CXR is useful as an initial screening tool and during acute exacerbations, but has limited sensitivity and specificity. Thin-section MDCT is the reference standard for diagnosis and quantification of bronchiectasis, providing detailed

Med Radiol Diagn Imaging (2016)
DOI 10.1007/174_2016_39, © Springer International Publishing Switzerland

morphological informations. Radiologists must know various causes of bronchiectasis, including common causes, such as recurrent infection or aspiration, and uncommon causes, such as congenital immunodeficiencies and disorders of cartilage development.

In industrialized countries, *inhalational exposures* to various toxicants are commonplace. Most acute toxic inhalations come from industries, home, and recreational sources. In addition to individual susceptibility, the characteristics of inhaled substances such as water solubility, size of substances, and chemical properties may affect disease severity as well as its location. A detailed history becomes even more important in such a patient and may help make a difference in the often chaotic setting of the emergency department. Laboratory evaluation, arterial blood gas analysis, and supportive measures, including the ABCs (airway, breathing, and circulation), may be required. Unfortunately, the varied presentations result in a nonspecific clinical syndrome and make diagnosis somewhat difficult. Despite substantial limitations, imaging can help in showing diffuse interstitial, alveolar, or mixed infiltrates, segmental consolidation, hyperinflation, pneumothorax, and pleural effusion. Thin-section MDCT can be used to further characterize lung abnormalities and continues to demonstrate previously unidentified characteristics that shape our understanding of noxious inhaled toxicant injury.

Table 1 Main conditions associated to airway obstruction

Malignant	Nonmalignant
Primary endoluminal carcinoma	Lymphadenopathy
Bronchogenic	Sarcoidosis
Adenoid cystic	Infectious (i.e., tuberculosis)
Mucoepidermoid	Vascular
Carcinoid	Sling
Metastatic carcinoma to the airway	Cartilage
Bronchogenic	Relapsing polychondritis
Renal cell	Granulation tissue from:
Breast	Endotracheal tubes
Thyroid	Tracheostomy tubes
Colon	Airway stents
Sarcoma	Foreign bodies
Melanoma	Surgical anastomosis
Laryngeal carcinoma	Granulomatosis with polyangiitis
Esophageal carcinoma	Pseudotumor
Mediastinal tumors	Hamartomas
Thymus	Amyloid
Thyroid	Papillomatosis
Germ cell	Hyperdynamic
Lymphadenopathy	Tracheomalacia
Associated with any of the above malignancies	Bronchomalacia
Lymphoma	Webs
	Tuberculosis
	Sarcoidosis
	Goiter
	Mucus plug
	Vocal cord paralysis
	Epiglottitis
	Blood clot

1 Acute Lower Airway Obstruction and Aspiration

1.1 Introduction

Acute obstruction of the central airway is an emergent situation that results from a wide variety of malignant and benign disease processes (Table 1). Acute management involves establishing a secure and patent route for adequate gas exchange. This requires rapid determination of the location of the obstruction and nature of the obstruction followed by a thoughtful management approach based on findings. Large airway obstruction typically presents with dyspnea and wheeze (particularly during exertion and with forced exhalation maneuver), and it is commonly mistaken for refractory exacerbations of COPD; variable intrathoracic upper airway obstruction is often caused by tracheobronchomalacia, an aspirated object, or central airway tumor. Complete airway obstruction (Fig. 1) is

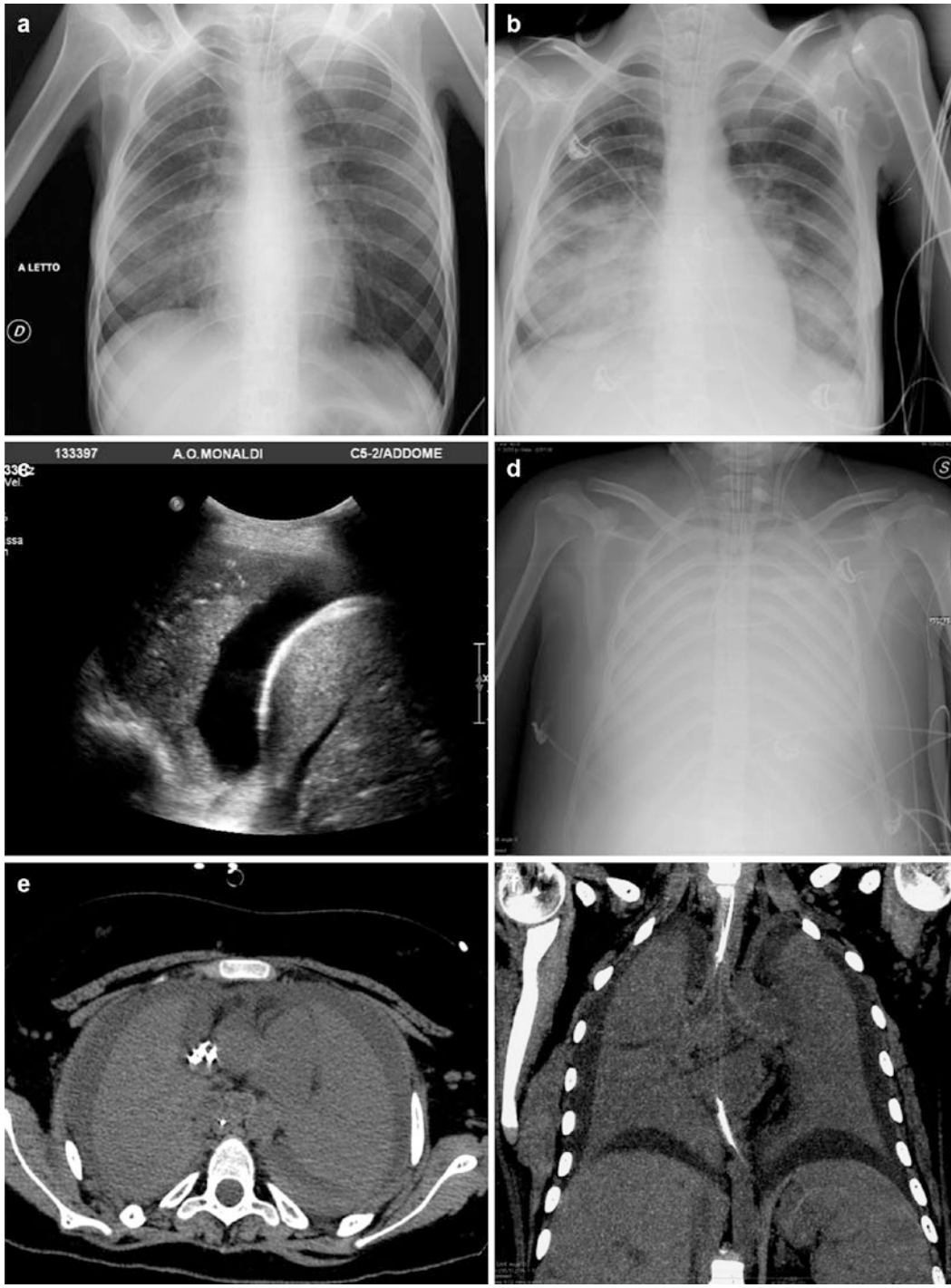

Fig. 1 Acute complete lower airway obstruction by rapid and severe course of toxic shock syndrome (TSS) in MRSA fatal progressive pneumonia. A 26-year-old menstruating woman with high fever, rash, hypotension, and rapidly evolving multiorgan failure is immediately transferred from ED into the ICU. (**a**) CXR at the admission in the ICU shows right lower lobe opacity. (**b**) Follow-up CXR 24 h later shows a new contralateral basal opacity. (**c**) Bedside longitudinal right LUS shows low right lobe complete consolidation associated to pleural effusion. (**d**) Patient in extracorporeal membrane oxygenation (ECMO). Twenty-four hours later, follow-up CXR shows completely opacified lungs. (**e**, **f**) Unenhanced MDCT axial and coronal MIP reconstructions show bilateral complete lung consolidation associated to pleural effusion. Note hypodense material that fills large airways

the worst scenario and will result in respiratory failure followed by cardiac arrest in a matter of minutes, a situation that requires an immediate, aggressive response, but it is, fortunately, very uncommon (Fig. 2).

1.2 Imaging

Patients with an acute upper airway complaint need to have their breathing issues addressed before being transferred to the radiology suite for

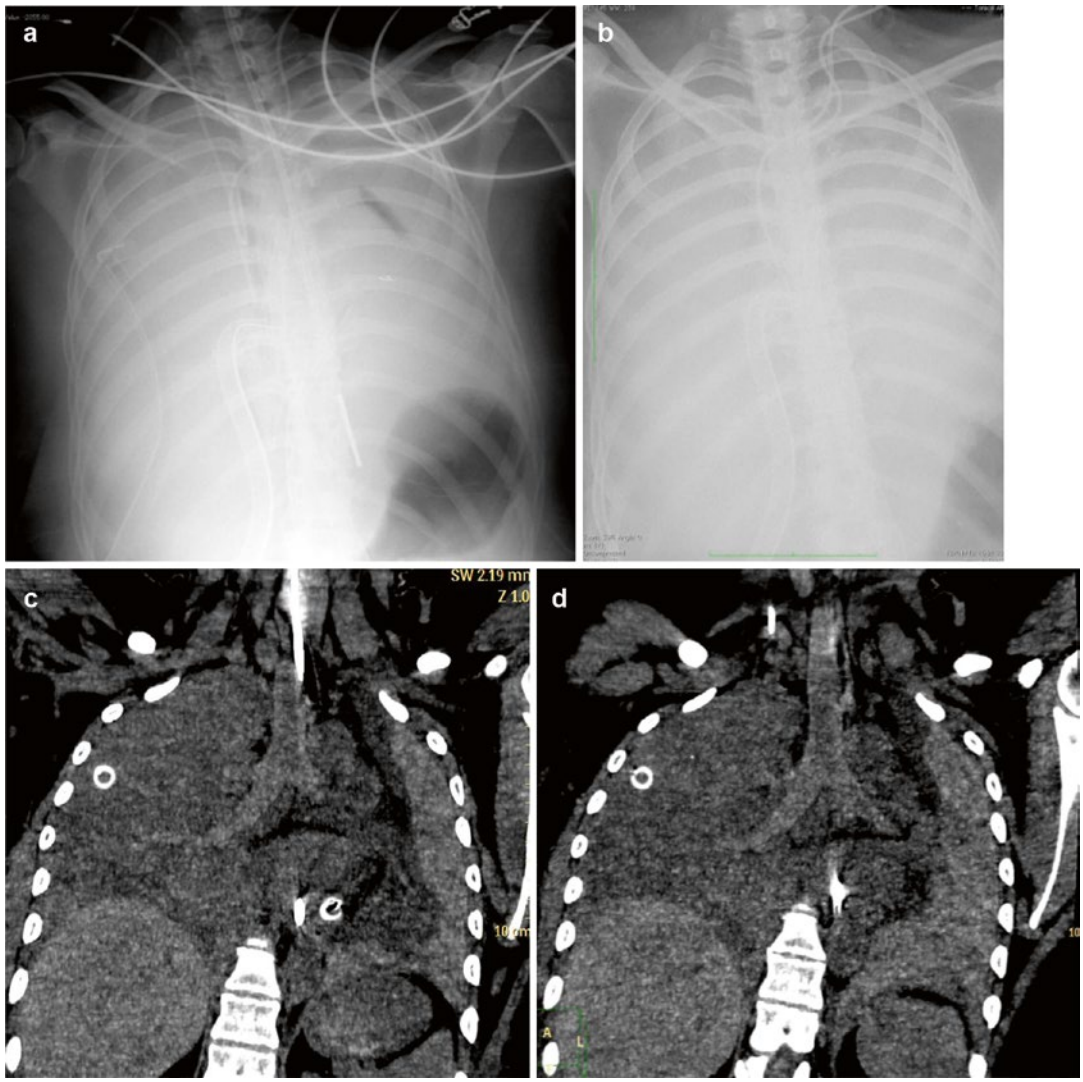

Fig. 2 Acute lower complete airway obstruction in a 16-year-old male with bleeding diathesis by treatment with anticoagulant therapy, abrupt massive postnasal bleeding, and airway hemorrhage by an highly vascularized bleeding nasopharyngeal angiofibroma.(**a**) CXR after nasogastric tube and right pleural drainages placement shows subtotal opacified lungs. (**b**) The patient was immediately transferred from ED into the ICU and CXR showed total opacified lungs.(**c**, **d**) Emergent unenhanced MDCT coronal reconstructions show hyperdense blood material that fills airways and the bloody hyperdensity mainly in the left lung (compare with Fig. 1). After nasopharyngolaryngoscopy, this patient was treated by emergent preoperative embolization. Juvenile nasopharyngeal angiofibroma is a benign, highly vascular hamartoma that arises from the nasopharynx almost exclusively in adolescent males

imaging. Intubation should be considered before any examination that requires patients to be supine (i.e., CT and MR imaging), especially if there is any suspicion of anaphylaxis or other difficulties in maintaining oxygen saturation levels. Portable anteroposterior (AP) chest radiography (CXR), complementary sonography (lung ultrasonography, LUS), and MDCT scanning of the neck and chest are the most effective initial emergent imaging studies to assess the location and extent of the airway obstruction. For patients who can tolerate lying flat for the study, MDCT provides the anatomic detail that permits planning of therapy. The study is assessed for location of primary tumor/mass, the degree of intrinsic versus extrinsic compression, and the length of the stricture. Furthermore, the relationship of the narrowing of the trachea relative to the larynx or the carina is readily assessed. For bronchial lesions, the extent of postobstructive atelectasis or infection is readily observed.

Flexible bronchoscopy provides a definitive view of the intraluminal disease but should be performed with preparation for management of the airway obstruction with laser, rigid bronchoscopy, or stent placement.

1.3 Pulmonary Parenchymal Abnormalities

Atelectasis, aspiration, airspace opacification or consolidations, air trapping and hyperinflation, hydrostatic pulmonary edema, and noncardiogenic pulmonary edema all present as pathological findings on CXR, LUS, and MDCT. Although it is often difficult, and sometimes impossible, to distinguish between these entities, certain radiographic features can aid in their diagnoses.

1.3.1 Obstructive Lung Diseases

Acute Exacerbation in Chronic Obstructive Pulmonary Disease

Chronic obstructive pulmonary disease (COPD) is defined as incompletely reversible expiratory airflow obstruction, likely caused by exposure to noxious inhaled particles (Rabe et al. 2007). The airflow limitation that underlies functional obstruction is usually progressive and associated with an abnormal inflammatory response of the lung. What is clinically called COPD reflects a complex syndrome encompassing potentially overlapping diseases such as pulmonary emphysema, chronic bronchitis, and small airway disease. Acute exacerbation of COPD is defined "as an event characterized by a change in the patient's baseline symptoms that is beyond normal day-to-day variations" is acute in onset and may warrant a change in regular medication in a patient with underlying COPD (Table 2) (Siafakas et al. 2004; Rabe et al. 2007). Three COPD phenotypes were identified based on morphologic CT changes and clinical features of COPD: phenotype A, characterized by no or minimal emphysema with or without bronchial wall thickening; phenotype E, characterized by emphysema without bronchial wall thickening; and phenotype M, characterized by emphysema with bronchial wall thickening (Fujimoto et al. 2006).

Acute Exacerbation in Asthma

Asthma is characterized by all of the following: (1) airway obstruction that is usually reversible, (2) chronic airway inflammation, and (3) nonspecific airway hyperreactivity.

The CXR features of asthma are not particularly specific, but the most common abnormality is *bronchial wall thickening*, with *hyperinflation* the second most common (identified up to 24 % though less reliable) finding (Lynch 1998). In patients with asthma, CT is indicated to identify

Table 2 Summary of diseases that provoke, precipitate, or mimic an acute COPD exacerbation (Siafakas et al. 2004)

Parenchymal diseases	Pneumonia and their complications; complicated bullae
Airway diseases	Bronchial carcinoma; tracheobronchial tree infections, common pollutant
Cardiac diseases	Congestive cardiac failure, right heart failure
Lung vessels	Pulmonary hypertension, acute embolism, hemoptysis
Pleura	Pleural effusion, pneumothorax
Muscles	Muscular wasting
Mediastinum	Pneumomediastinum

suspected complications, particularly allergic bronchopulmonary aspergillosis, and mimics of asthma such as hypersensitivity pneumonitis. When it is performed, CT is helpful for evaluating the extent of airway thickening (remodeling: airway walls are thicker than healthy individuals and the degree of airway wall thickness directly correlates with the severity of airflow obstruction and clinical disease) (Aysola et al. 2008), bronchial dilation, and expiratory air trapping. Air trapping is usually defined as the percentage of the lung less than 850 HU on expiratory CT, and those individuals with an air-trapping percentage above the median value of 9.66 % defined as having an air-trapping phenotype. Bronchial dilation, or bronchiectasis (defined as a bronchus with a larger diameter than the internal diameter of the adjacent pulmonary artery), is more prevalent in asthmatic patients than in healthy subjects. Acute complications of asthma may include pneumothorax, pneumomediastinum (and rarely pneumopericardium, pneumoperitoneum, pneumoretroperitoneum, pneumorrhachis, and even subdural emphysema), mucus impaction with or without atelectasis, and pneumonia (Woods and Lynch 2009).

1.3.2 Consolidations or Airspace Opacifications or Alveolar Opacity or Alveolar Pattern

Consolidation is the most common cause of pulmonary opacities in the acute airway obstruction population. In contrast to ground-glass opacities (GGO), consolidation obscures underlying vascular structures and frequently is associated with absence of volume loss and air bronchograms by opacification of lung acini with little or no involvement of conducting airways. By definition, diseases that produce consolidation are characterized by a replacement of alveolar air by fluid, cells, tissue, or some other substances (Hansell et al. 2008). If acute, consolidation is most commonly caused by pulmonary edema (of both cardiogenic and noncardiogenic causes), pulmonary hemorrhage, acute eosinophilic pneumonia, acute extrinsic allergic alveolitis, radiation pneumonitis, pulmonary infarction, or infectious pneumonia (Table 3).

Table 3 (**a**) Diseases recognized as causing alveolar opacity or pattern

Transudate
Hemodynamic pulmonary edema[a]
Non-hemodynamic pulmonary edema
Diffuse alveolar damage (ARDS)[a]
Exudate
Infective pneumonia[a]
Eosinophilic pneumonia
Lipoid pneumonia
Hemorrhage
Diffuse alveolar hemorrhage (DAH)
Severe cardiac failure[a]
Pulmonary infarction[a]
Emboli[a]
Thromboembolism[a]
Fat embolism
Amniotic fluid embolism
Bone marrow embolism
Infiltration
Adenocarcinoma ex-bronchoalveolar cell carcinoma
Lymphoma
Miscellaneous
Pulmonary alveolar proteinosis
Acute extrinsic allergic alveolitis
Sarcoidosis
Radiation pneumonitis

[a]See other chapters of the book

Table 3 (**b**) Imaging signs of acute obstruction of airways by alveolar disease

1. Acinar or peribronchiolar nodules
2. Air alveologram and bronchiologram
3. Air bronchogram
4. Butterfly or "bat's wing" distribution
5. Coalescence (early)
6. Fluffy, ill-defined margins
7. Perihilar, diffuse, segmental, or lobar distribution
8. Present soon after onset of symptoms; rapid change

1.3.3 Thoracic Oncologic Emergencies

Oncologic patients often experience emergent complications that are either direct result of the underlying malignancy or an indirect result related to the therapy (Table 4).

Airway obstruction complicates approximately 20–30 % of patients with lung cancer, and large masses that compress the central airways may

Table 4 Thoracic oncologic direct and indirect complications

Oncologic direct complications	
Mass effect and airway compromise	Airway occlusion Tracheo- or broncho-esophageal fistula
Mass effect and vascular invasion	SVC obstruction, SVC syndrome
Mass effect and invasion of cardiac chambers	Pericardial effusion and cardiac tamponade Tumor extension into the cardiac chambers
Pleural involvement	Massive pleural effusion, hemothorax, pneumothorax Chylothorax
Neovascularity	Massive hemorrhage, pseudoaneurysm, or AV fistula
Systemic manifestations	Massive pulmonary embolism, disseminated intravascular coagulation, opportunistic infections
Oncologic indirect complications	
Postoperative or post-procedural	Pneumothorax, massive hemorrhage, hemothorax, complications of vascular injury, bronchopleural fistula
Postradiation complications	Airway edema and obstruction Radiation pneumonitis, fistula formation
Chemotherapy-related complications	Spontaneous pneumothorax, immunosuppression and opportunistic infections, fistula formation

SVC = superior vena cava; AV = arteriovenous

result in postobstructive atelectasis or pneumonia and airway compromise. Rapidly growing tracheal, mediastinal, and hilar masses are most common causes (Fig. 3) (Quint 2009; Guimaraes et al. 2014). Knowledge of airway narrowing is important before attempting percutaneous and surgical biopsy because it may lead to collapse of residual normal lung and sudden respiratory decompensation (McCurdy and Shanholtz 2012). Muscle relaxant drugs used during anesthesia may precipitate dangerous respiratory compromise in patients with pre-existing airway compression by tumor owing to loss of chest wall tone.

1.3.4 Noncardiogenic Pulmonary Edema (NCPE)

Lung edema includes (1) hydrostatic edema caused by increased capillary pressure or decreased oncotic pressure, (2) ARDS (permeability edema caused by DAD resulting in interstitial and alveolar fluid accumulation), (3) permeability edema without alveolar damage (such as heroin-induced edema, edema following cytokine administration, and high-altitude edema) primarily resulting in interstitial fluid accumulation, and (4) mixed forms of hydrostatic and permeability edema (such as neurogenic edema, reperfusion and re-expansion edema, edema following lung transplantation, etc.)

1.3.5 High-Altitude Pulmonary Edema (HAPE)

High-altitude illness includes the cerebral syndromes of acute mountain sickness (AMS), high-altitude cerebral edema (HACE), and the pulmonary syndrome of high-altitude pulmonary edema (HAPE), recognized as an alveolar fluid accumulation in unacclimatized individuals by Houston in 1960 and attributed solely to high-altitude exposure (Houston 1960); it is mainly seen in children or young adults who rapidly ascend to heights of 2000–3500 m or greater and typically occurs 3–48 h after ascent, with the hallmark symptom being dyspnea at rest, often associated to dry or with frothy pink sputum production cough and restlessness. Approximately 50 % of patients with HAPE also show symptoms of AMS/HACE, but these two forms of altitude illness can exist independently of each other (Bartsch et al. 2005). The mechanism remains unclear: HAPE is believed to be a form of non-cardiogenic pulmonary edema without alveolar damage caused by exposure to the low pO2 found at high altitudes. Hypoxia leads to uneven areas of vasoconstriction within the pulmonary vascular bed, resulting in a pattern of patchy overperfusion (Swenson et al. 2002); these foci of high vascular pressure lead to localized violation of the capillary endothelium, causing fluid extravasation. When available, CXR features initially are heterogeneous peripheral alveolar patchy, fluffy infiltrates progressing eventually to widespread, confluent airspace involvement more severe in lung bases, but the pattern of distribution is usually unpredictable. Portable lung ultrasonography provides a more feasible imaging option in remote locations and shows progressively larger numbers of extravascular fluid

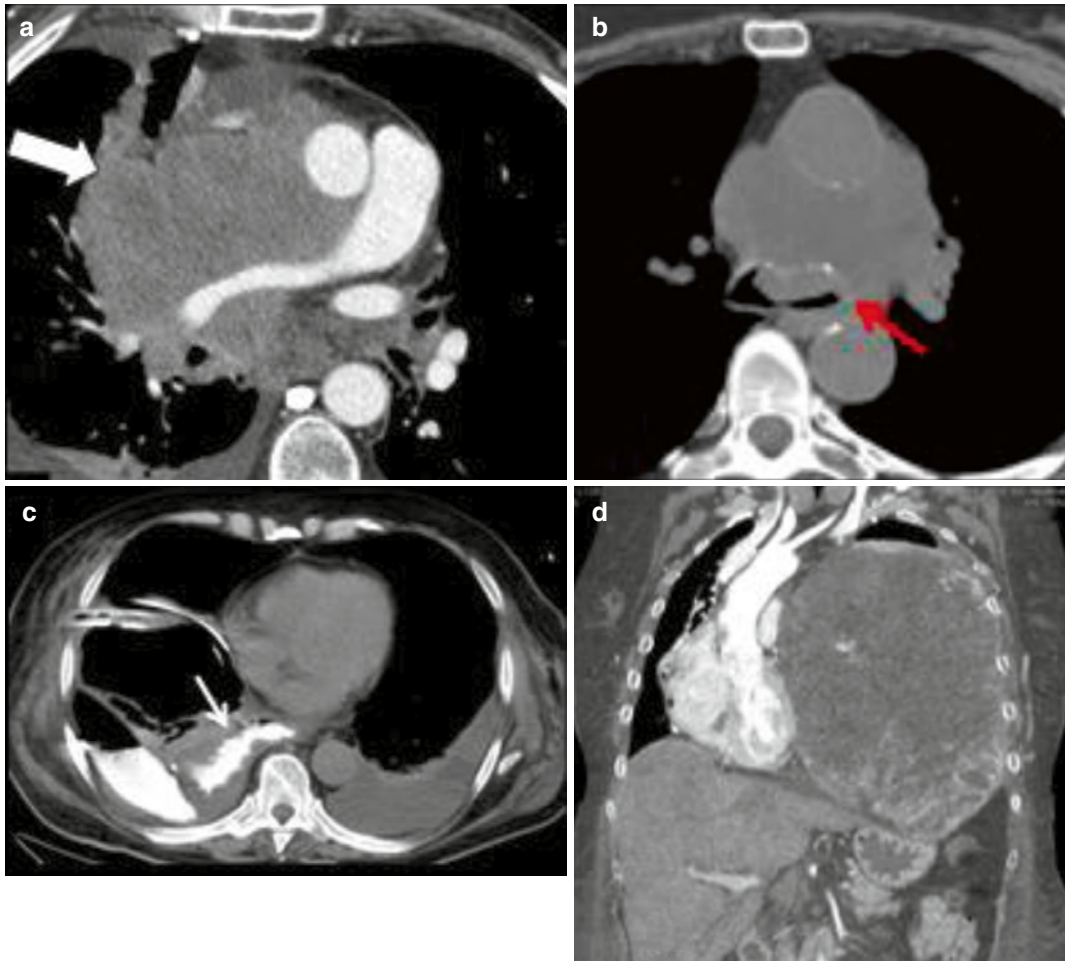

Fig. 3 MDCT of thoracic oncologic emergencies. (**a**) Lung small-cell carcinoma extending into the mediastinum with SVC syndrome (*white arrow*). (**b**) A soft tissue hilar mass with carinal and left bronchial extension (*red arrow*) in a known non-small cell carcinoma in a patient with acute breathlessness. (**c**) Esophageal carcinoma ruptured in right lung parenchyma and with esophago-pleural fistula (*white arrow*). (**d**) Mediastinal chondrosarcoma with rightward mediastinal shift and acute airway obstruction

comet tails in patients ascending to altitude and suffering from HAPE (Fagenholz et al. 2007; Pratali et al. 2010). The most modifiable risk factor for the development of HAPE is the rate of ascent to high altitude; the mainstay of therapy increases alveolar and arterial oxygen by descent or with supplemental oxygen. HAPE is a potentially life-threatening illness that is completely preventable; as the popularity of trekking and climbing grows among the general population, physicians will be increasingly relied on as a source of education, prophylaxis, and treatment, making a working familiarity with altitude-induced illnesses such as HAPE an indispensable tool for emergency physicians.

1.3.6 Neurogenic Pulmonary Edema (NPE)

A number of intracranial conditions, including head trauma, hemorrhage (usually subarachnoid), tumors, and encephalitis, can be associated with acute pulmonary edema. It can occur within a minute to hours following a neurologic insult and usually resolves within 72 h. Patients may present with varying degrees of dyspnea, tachypnea, and cyanosis shortly after suffering the brain insult. The onset of symptoms occurs in <4 h in the majority and death in 10%. The mechanism is unclear: it has been suggested that a sudden burst of neural activity stimulates the sympathetic nervous system and an adrenergic

response leading to increased extravascular lung water, increased pulmonary hydrostatic pressure, and increased lung capillary permeability (Tan and Lai 2007). The CXR picture is indistinguishable from that of cardiogenic PE (nonspecific, bilateral, rather homogeneous airspace consolidative appearances with an apical predominance are present in about half of cases) except that the heart is not enlarged and it can take up to 24 h to be apparent on imaging (Fig. 4). Radiologic findings in neurogenic pulmonary edema also disappear within 1–2 days, thereby confirming the absence of any associated DAD (Gluecker et al. 1999).

1.3.7 Re-expansion Edema (REPE)

The condition occurs often in young patients in the setting of rapid expansion of a collapsed lung, with acute-onset shortness of breath usually occurring within hours of re-expansion. The onset of pulmonary edema can be delayed by up to 24 h in some cases (Echevarria et al. 2008). It occurs following approximately 1 % of pneumothorax re-expansions or thoracentesis procedures (mostly if large-volume drainage >3 l). Although the exact mechanism of REPE has not been identified, it appears to be caused by multiple mechanisms. Increased capillary permeability due to hypoxic injury, reperfusion injury with release of toxic

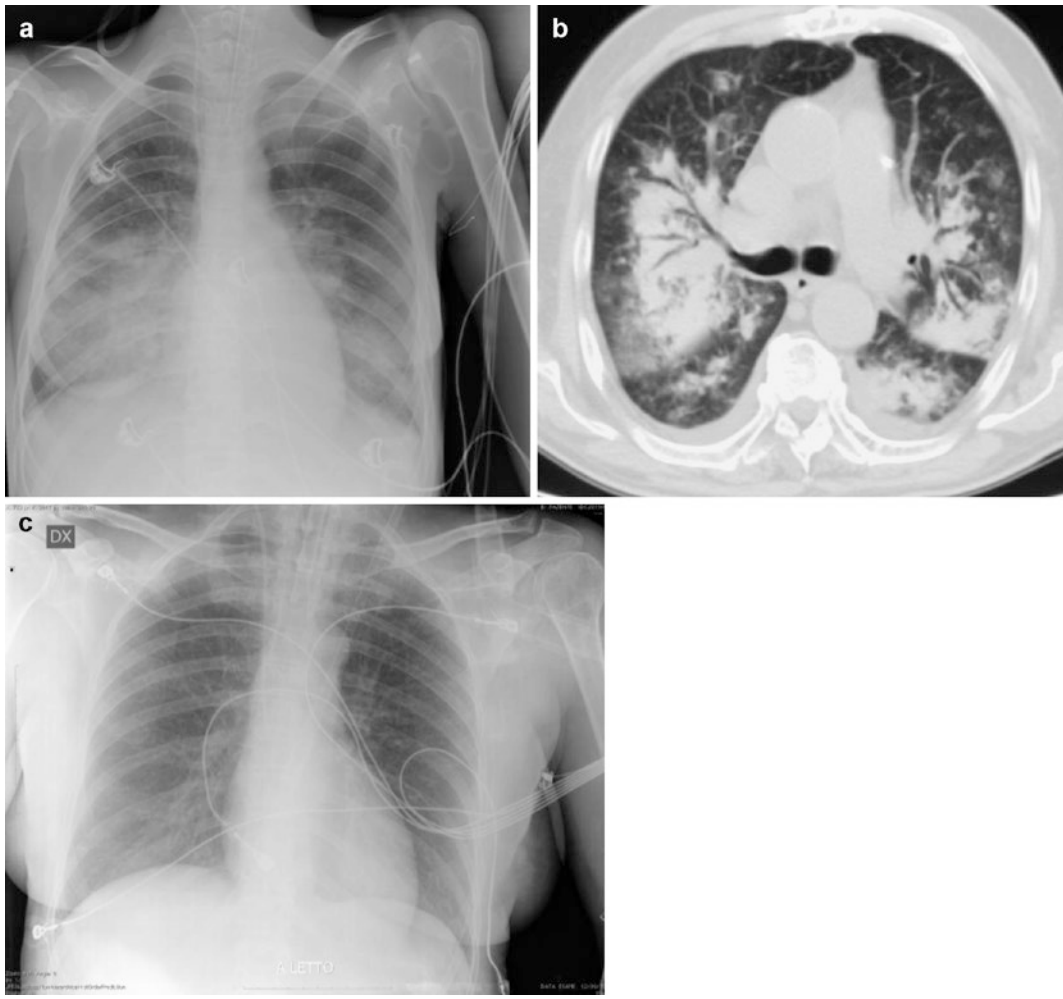

Fig. 4 Neurogenic pulmonary edema. (**a**) Anteroposterior bedside CXR view shows bilateral alveolar opacities in a 54-year-old woman with shortness of breath and subarachnoid hemorrhage, who developed neurogenic pulmonary edema. (**b**) MDCT axial scan shows diffuse bilateral and symmetric patchy ground-glass and consolidative opacities sparing the lung periphery. (**c**) Follow-up CXR 3 days later shows normal findings

oxygen free radicals, and surfactant depletion are all thought to play a major role. Furthermore, a delay in lymphatic return by stasis during prolonged collapse and bronchial occlusion may also partly account for the development of REPE. It can progress for 24–48 h and usually shows slow resolution over 5–7 days. REPE may lead to severe hypoxemia, which will increase lung damage and may result in extensive adult respiratory distress syndrome (ARDS) and multiorgan failure. CXR findings are alveolar opacities usually unilateral in those portions of the lung that were previously collapsed; rarely edema can develop in the contralateral lung (Baik et al. 2010). Thin-section MDCT findings of REPE are peripheral patchy areas of GGO frequently combined with consolidation as well as interlobular septal and intralobular interstitial thickening (Fig. 5). The British Thoracic Society guidelines suggest that less than 1.5 l of pleural fluid be drained at a time (BTS Pleural Disease Guideline 2010). Drainage catheters can be intermittently plugged to prevent rapid lung re-expansion. Rapid re-expansion of pneumothoraces is less easily controlled and caution should be taken to avoid high negative intrapleural pressures.

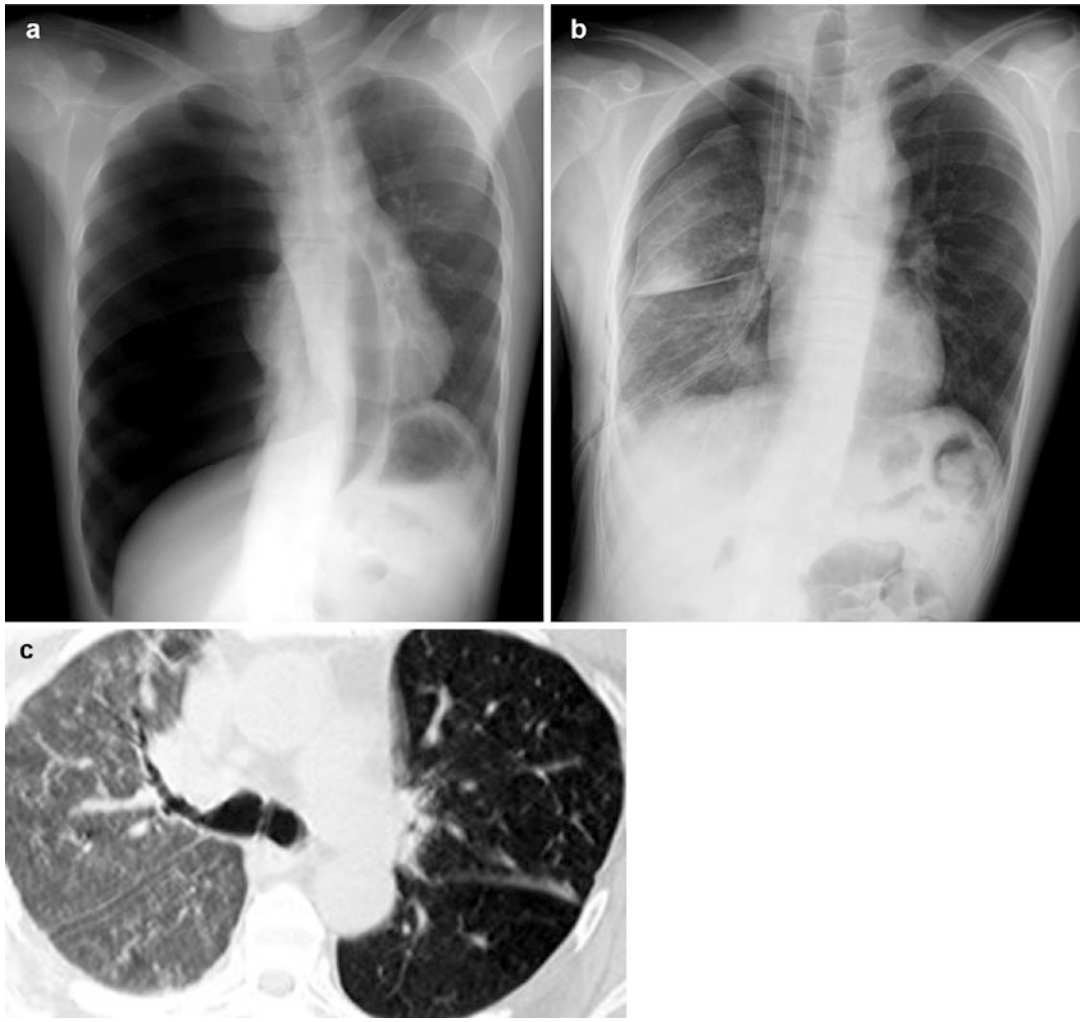

Fig. 5 Re-expansion pulmonary edema. (**a**, **b**) Standard erect PA CXR shows right lung re-expansion pulmonary edema following a spontaneous pneumothorax drainage. (**c**) Thin-section low-dose MDCT scan shows unilateral diffuse ground-glass opacity

1.3.8 Atelectasis

Atelectasis or *collapse* (Hansell et al. 2008), a decrease in lung volume accompanied by increased opacity (CXR) or attenuation (CT scan) in the affected part of the lung, is a common cause of pulmonary opacities in the acute airway obstruction population. One of the commonest mechanisms is resorption of air distal to airway obstruction (e.g., an acutely complicated endobronchial neoplasm or foreign body). Atelectasis can mimic pneumonia, particularly when signs of volume loss, such as crowding of air bronchograms, fissural deviation, mediastinal shift, and diaphragmatic elevation, are absent. Flat, platelike opacities are characteristic of discoid atelectasis. Complete lung collapse, lobar collapse, or segmental collapse can also be seen. The characteristic LUS finding is a homogenous, well-demarcated hyperechoic lung consolidation. In comparison with pneumonia, no air bronchograms are usually visible. The size of the lung consolidation may vary during the breathing cycle due to ventilation. Atelectasis is categorized according to mechanism as obstructive, compressive, cicatricial, and adhesive.

1.4 Acute Aspiration

The term *aspiration* describes a variety of situations involving the intake of solid or liquid materials into the airways and lungs (Franquet et al. 2000). The clinical and radiologic manifestations are protean, varying from asymptomatic focal inflammatory reaction with few or no radiologic abnormalities to severe life-threatening disease (Table 5).

Alcoholism is probably the most important predisposing factor for pulmonary liquid aspiration in adults, although other factors (e.g., general anesthesia, loss of consciousness, structural abnormalities of the pharynx and esophagus, neuromuscular disorders, deglutition abnormalities) may also contribute to aspiration.

Aspiration can result in airway obstruction, chemical pneumonitis, or infectious pneumonia, depending on the volume and type of aspirate. Patchy, ill-defined ground-glass, consolidative, and nodular opacities are the most frequently encountered radiographic manifestations of aspiration. Opacities typically appear rapidly and are most commonly located in the dependent regions of the lungs: the posterior segment of the upper lobes and the superior and posterior basal segments of the lower lobes (Franquet et al. 2000). Opacities may increase in conspicuity over the first 1–2 days in aspiration pneumonitis, but should resolve relatively rapidly thereafter. If opacities persist or increase over several days, aspiration pneumonia is likely present. Patchy, dependent ground-glass, and consolidative opacities are also seen on CT. "Tree-in-bud" opacities result from filling and inflammation of the distal airways (Rossi et al. 2005). When tree-in-bud opacities are present in a dependent distribution, they are highly suggestive of aspiration (Fig. 6).

Table 5 Main syndromes of acute/recurrent pulmonary aspiration

Aspirated material	Clinical effects	Imaging findings
Foreign bodies	Bronchial obstruction	Atelectasis Hyperinflation Abscess
Water	(Near) drowning	Airspace opacity
Gastric contents (Mendelson syndrome)		
Acute	Chemical pneumonitis, anaerobic infection, lung abscess	Airspace opacity Cavity
Chronic/recurrent	Recurrent aspiration Bronchiolitis Bronchiectasis	Migratory opacities Centrilobular nodules/air trapping
Acute exogenous		
Lipoid pneumonia (fire-eater hydrocarbon pneumonia)	Chemical pneumonia	Consolidations Pneumatoceles Masses

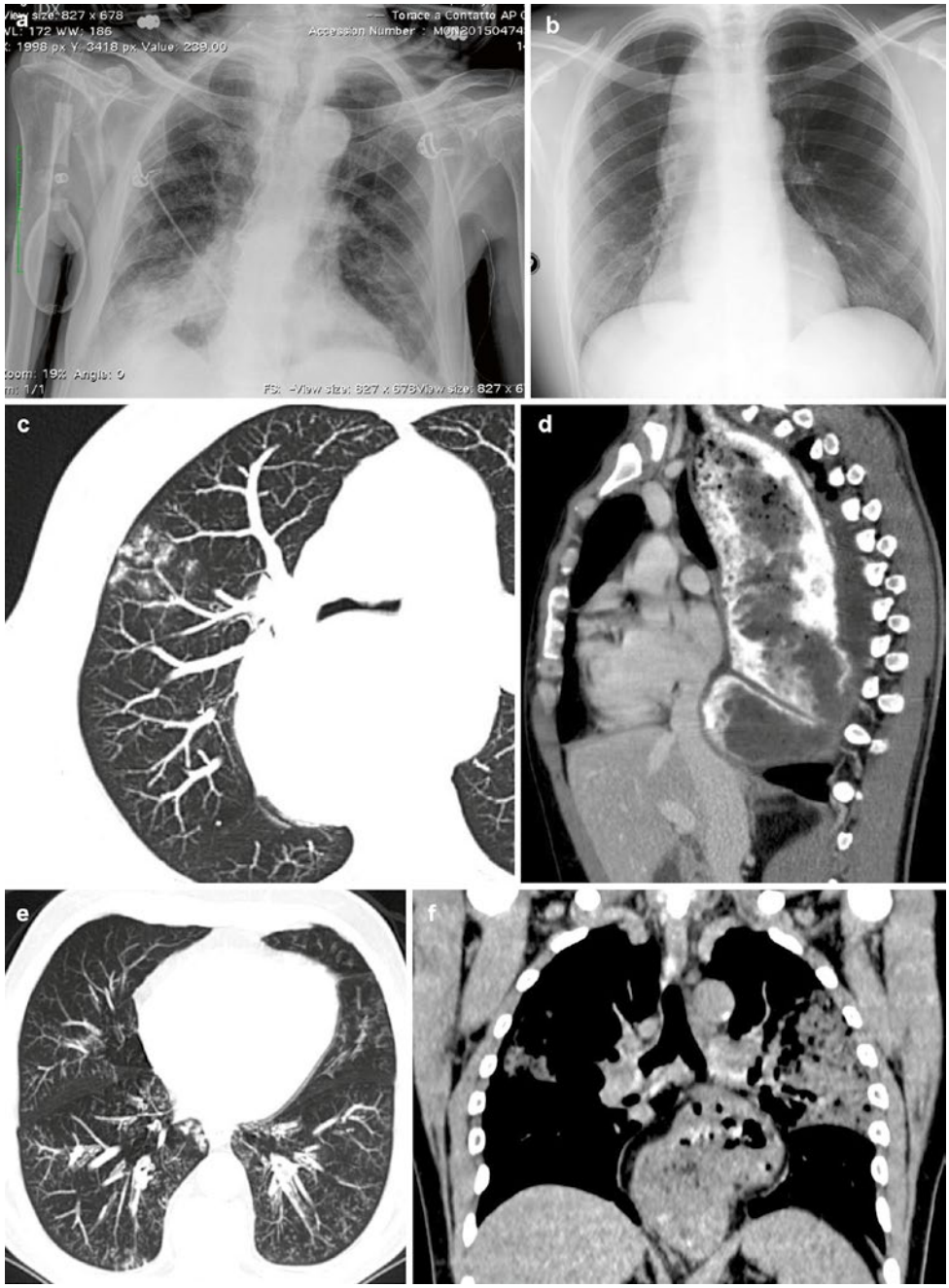

Fig. 6 Case 1. Acute aspiration pneumonia (Mendelson syndrome) in a 65-year-old man who had undergone surgery for intestinal obstruction. (**a**) Anteroposterior CXR view obtained 2 h after surgery demonstrates a focal consolidation in the right lower lobe, a finding that is consistent with aspiration pneumonia. Case 2. Aspiration bronchiolitis in a 57-year-old man with esophageal achalasia. (**b**) Frontal CXR view shows a right superior and middle paramediastinal mass. (**c**) Thin-section MDCT axial scan shows multiple diffuse centrilobular areas of increased attenuation with a characteristic tree-in-bud appearance (aspiration bronchiolitis); note that dilated esophagus displaces tracheal carina. (**d**) MDCT sagittal reconstruction shows typical findings of achalasia with contrast medium-filled esophagus, marked esophageal dilatation, and anterior bowing of the trachea. Case 3. Aspiration bronchiolitis and lung consolidations in a 46-year-old man with hiatal hernia. (**e**, **f**) Axial and coronal MDCT reconstruction shows centrilobular nodules, tree-in-bud pattern in lower lobes, consolidations in upper lobes, and large gastric hernia

1.4.1 Foreign Body Aspiration

Aspirated foreign bodies are by far the most common cause of intraluminal airway abnormalities in childhood, unusual in adults, and often overlooked as a cause of airway obstruction (Yadav et al. 2007). Up until age 15, both right and left main bronchi arise at about the same angle from the trachea so that objects may be aspirated into either side; afterward, the right main bronchus arises in a less acute, more straight path than the left (Kosucu et al. 2004). The most frequently aspirated foreign bodies are food (especially nuts), teeth, dental devices, and medical instruments, and 70 % will be nonopaque on conventional radiography (Fig. 7).

Some nuts, such as peanuts, have an oil that leads to inflammation and edema making them more difficult to expel. When a foreign body enters the lung parenchyma, prolonged irritation with intermittent infections may cause massive hemoptysis. At radiology, an aspirated foreign body may cause one lung or lobar/segmental overinflation or atelectasis (obstructive emphysema) with chronic volume loss in the affected lobe, mediastinal shift, pneumomediastinum, recurrent pneumonias, and bronchiectasis; it can occasionally mimic a congenital malformation or neoplasm (Fig. 8).

If the patient is clinically able, an expiratory CXR may demonstrate air trapping on the affected side by lack of collapse of the lung and shift of the mediastinum away from the side with the foreign body. If the patient is a child or otherwise not able to cooperate for an expiratory study, a decubitus view of the chest, with the suspected side down, may show a lack of collapse of the air-trapped lung. CT may demonstrate the foreign body and is far more sensitive than CXR in

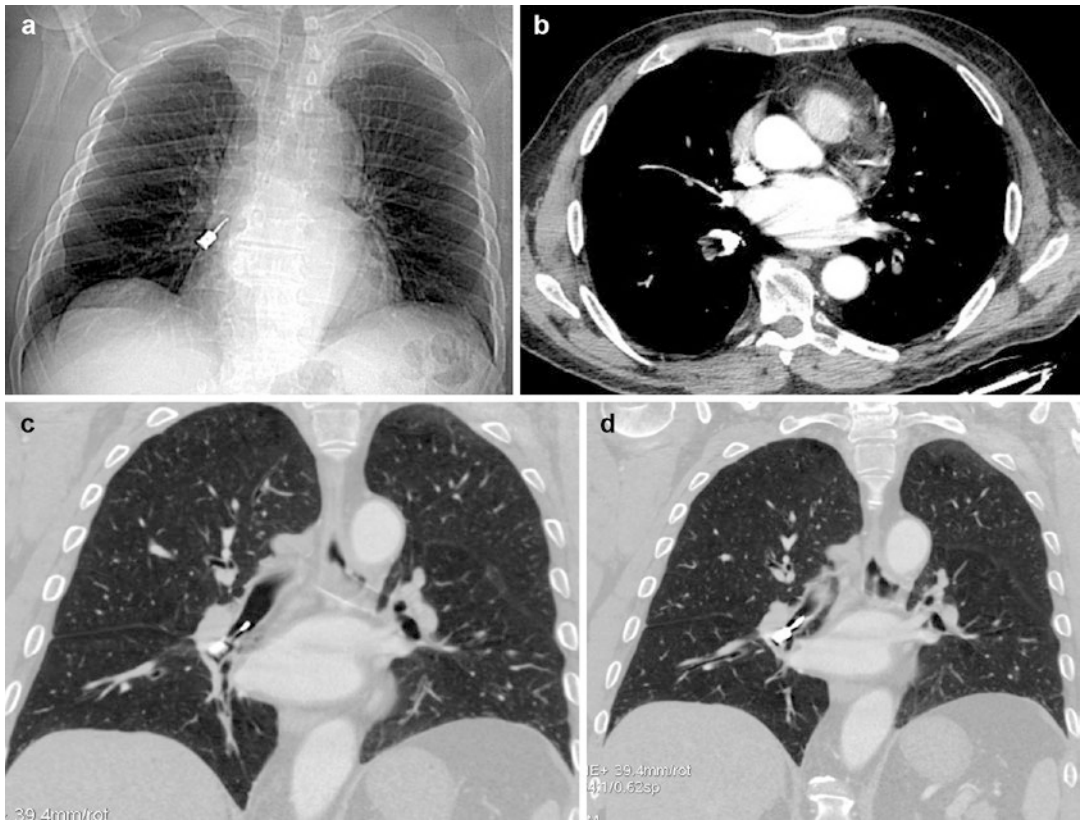

Fig. 7 Post-aspiration imaging in a 70-year-old alcoholic man. MDCT (**a**) scanogram and (**b**) axial and (**c**, **d**) coronal reconstruction images clearly show inhalation of a metallic foreign body (dental screwdriver), located in the right lower lobe bronchus

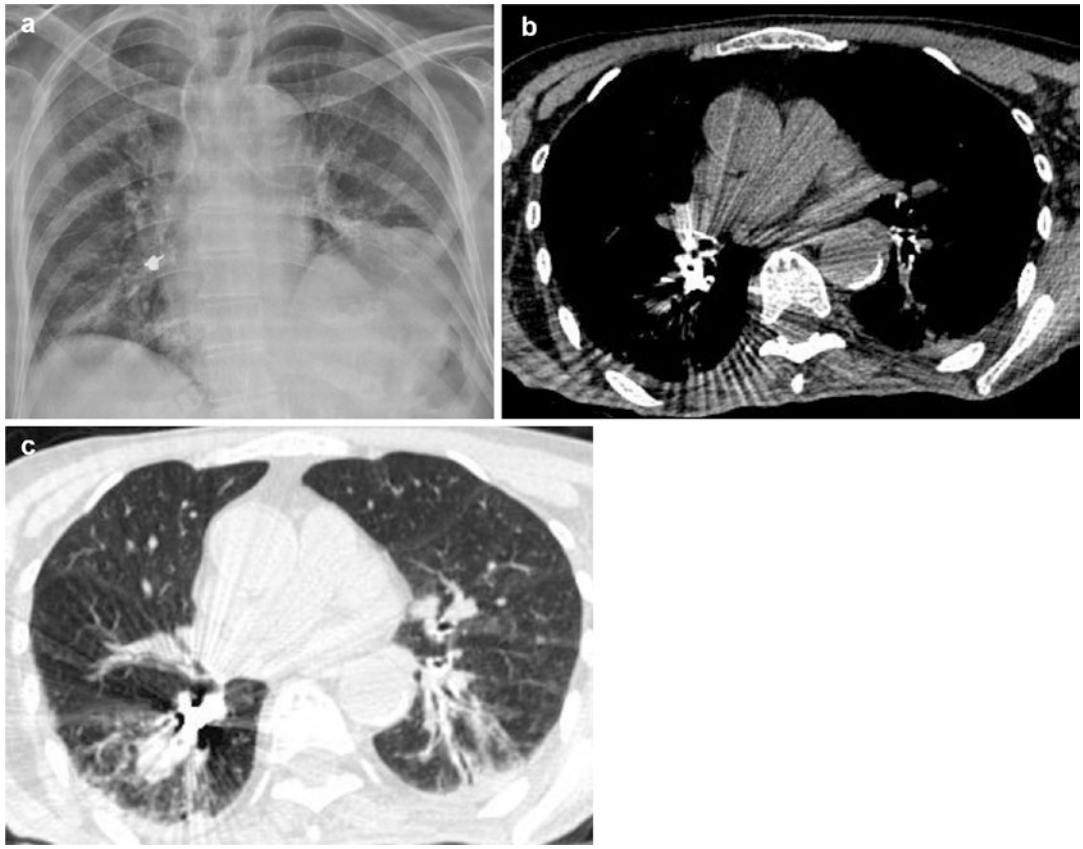

Fig. 8 Post-aspiration imaging in a 79-year-old woman. (**a**) CXR and MDCT with (**b**) mediastinal and (**c**) parenchymal windows show a foreign body inhalation, again located in the right lower lobe bronchus (earring)

demonstrating subtle low-attenuation intrabronchial material (Fig. 9) (Zissin et al. 2001).

1.4.2 Drowning or Near Nonfatal Drowning

Drowning is a process resulting in primary respiratory impairment from submersion in a liquid medium (Idris et al. 2003) and may be either a fatal or nonfatal event (Szpilman et al, 2012). Deaths because of drowning have estimated approximately 305,000 deaths in 2008 (WHO 2011). Young children are at particularly high risk of drowning, and males in general face a significantly greater risk than females. Drowning may be further classified as cold-water (<20 °C) or warm-water injury (>20 °C). The most important contributory factors to morbidity and mortality from drowning are hypoxemia and acidosis and the multiorgan effects of these processes. Central nervous system (CNS) damage may occur because of hypoxemia sustained during the drowning episode (primary injury) or may result from arrhythmias, ongoing pulmonary injury, reperfusion injury, or multiorgan dysfunction (secondary injury), particularly with prolonged tissue hypoxia. After initial breath holding, when the victim's airway lies below the liquid's surface, an involuntary period of laryngospasm is triggered by the presence of liquid in the oropharynx or larynx (stage 1, "dry drowning"). At this time, the victim is unable to breathe in air, causing oxygen depletion and carbon dioxide retention. In stage 2, the victim still usually presents with laryngospasm but may begin to swallow water into the stomach. As the oxygen tension in blood drops further, laryngospasm releases, and

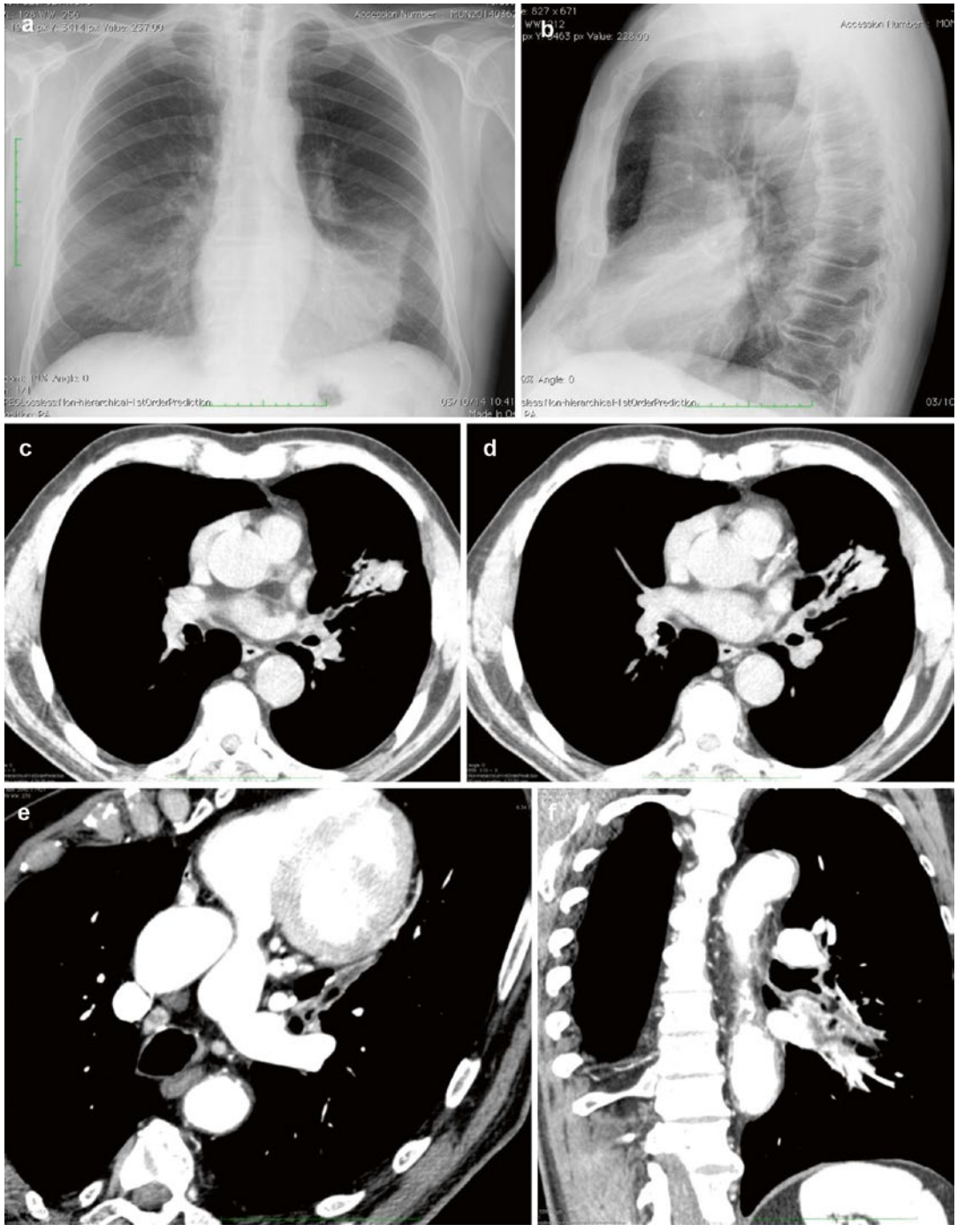

Fig. 9 Postobstructive atelectasis in a 46-year-old man who had inhaled vegetable lipid matter. (**a**) Posteroanterior and (**b**) latero-lateral CXR views show segmental lingular lung collapse, without evidence of foreign body. (**c**, **d**) Axial MDCT scans confirm lingular collapse and show possible endoluminal oval hypodensity. MDCT (**e**) oblique axial and (**f**) coronal MIP reconstructions show a lipid-density oval endobronchial mass. At bronchoscopy foreign body aspiration diagnosis was confirmed and a vegetable lipid matter was removed

the victim gasps and hyperventilates, possibly aspirating variable amounts of liquid. This leads to further hypoxemia (stage 3). Ultimately, if the process of drowning is not interrupted, hypoxia progresses to the point of complete circulatory collapse and cardiac arrest (Tourigny and Hall 2012). Pulmonary infections may occur in a delayed fashion from aspirated material, some of which may result from rare or atypical pathogens such as fungi. Patients in cardiac arrest are more likely to display a nonshockable cardiac rhythm (i.e., asystole or pulseless electrical activity). Those who survive the initial resuscitation phase are at significant risk for developing serious delayed sequelae, such as ARDS, pancreatitis, disseminated intravascular coagulation, or rhabdomyolysis during their subsequent hospital stay. The acute aspiration of massive amounts of water produces a pulmonary edema that is radiographically indistinguishable from pulmonary edema from other causes (Hunter and Whitehouse 1974; Causey et al. 2000). The clinical significance of near drowning depends more on the volume of water aspirated than on whether the aspirate is

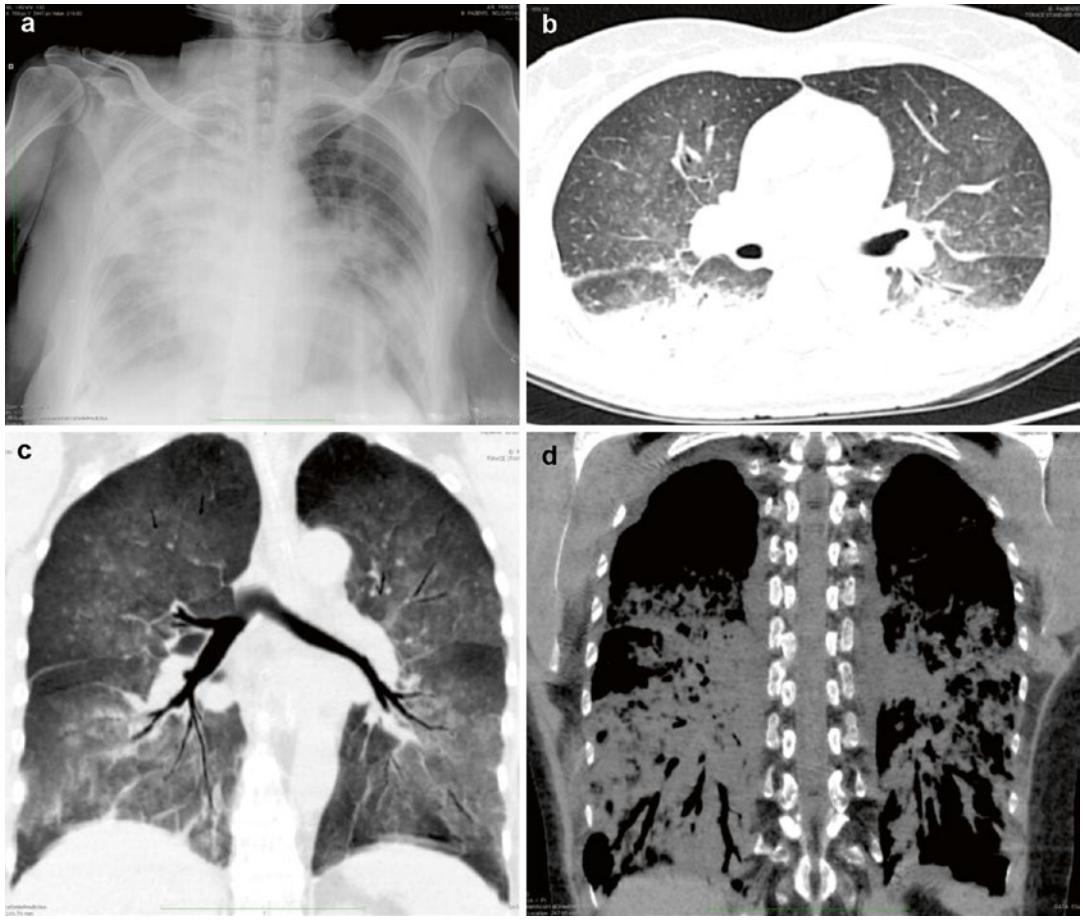

Fig. 10 Near drowning in a 67-year-old man who was admitted 3 h after nearly drowning in chlorinated water in an hotel pool. (**a**) CXR obtained at the time of admission reveals cardiac enlargement, diffuse confluent alveolar patterns of pulmonary edema, and peribronchial cuffing. Emergent MDCT (**b**) axial and (**c**, **d**) coronal reconstructions (parenchymal and mediastinal windows) show diffuse ground-glass and consolidative dependent abnormalities

freshwater or saltwater. Classic CXR findings in severe near drowning consist of alveolar edema with extensive "fluffy" areas of increased opacity that tend to coalesce throughout both lungs (Fig. 10). In mild near drowning, findings range from normal to confluent irregular peripheral areas of increased opacity in a subsegmental or segmental distribution with peripheral sparing. Pneumonia may be a complication of the aspiration of either fresh- or saltwater and, depending on the water source, may be caused by a variety of microorganisms including bacteria, fungi, and mycobacteria (Tourigny and Hall 2012).

1.4.3 Gastric Acid Aspiration (Mendelson Syndrome)

Vomiting with massive aspiration of gastric contents is a very frequent phenomenon; gastric acid with a pH <2.5 can cause pathologic reactions varying from mild bronchiolitis to hemorrhagic pulmonary edema. The posterior segments of the upper lobes and the superior segments of the lower lobes are the most frequently involved lung sites when the patient is recumbent. Acid liquid introduced into the airways is rapidly disseminated throughout the bronchial tree and lung parenchyma, producing a chemical pneumonitis within minutes. The magnitude of injury is directly related to the pH and volume of the aspirated material. The overall mortality rate associated with massive aspiration of gastric acid is approximately 30 % and is greater than 50 % in patients with initial shock or apnea, secondary pneumonia, or adult respiratory distress syndrome (Bynum and Pierce 1976). Classic CXR findings in acute gastric acid aspiration include bilateral perihilar, ill-defined, alveolar consolidations, multifocal patchy infiltrates, and segmental or lobar consolidation, which are usually localized to one or both lung bases (Fig. 6a).

1.4.4 Acute Exogenous Lipoid Pneumonia (Fire-Eater Pneumonia)

Exogenous lipoid pneumonia is a rare condition caused by inhalation or aspiration of plant, animal, or mineral fats and may take an acute or chronic form. Acute form is usually associated with accidental poisoning in children; in an adult population, it typically occurs in fire-eaters, who use oily substances in their shows (Betancourt et al. 2010). Clinically, acute lipoid pneumonia presents most often with cough, dyspnea, and fever. CXR pictures show consolidation, reticular and mixed alveolar-interstitial changes, as well as nodular lesions. Other rarer abnormalities, which may be noted on radiograms, are pneumatocele, pneumothorax, pneumomediastinum, and pleural effusion (Franquet et al. 2000). Most commonly, CT shows areas of a negative attenuation coefficient (between −150 and −30 HU) consolidation and ground-glass opacities as well as interstitial changes such as interlobular septal thickening and intralobular lines; fine, poorly demarcated centrilobular nodules and nodular lesions; pneumatocele; pneumothorax; pneumomediastinum; and pleural effusion (Brander et al. 1992; Laurent et al. 1999). Changes involve one or both lungs and are usually located in lower lobes or in the right middle lobe and may be multifocal or bilateral (Fig. 11).

1.5 Summary

Airway obstruction is an uncommon but potentially life-threatening condition that can be due to a number of malignant and benign processes; the diagnosis is based on the combination of characteristic findings on physical examination, as well as physiological, imaging, and endoscopic studies. Ultimately, the diagnosis is made by direct visualization of the tracheobronchial obstruction by bronchoscopy. Significant airway obstruction presenting with imminent suffocation requires immediate action to promptly and effectively reestablish and secure a patent airway and relieve the obstruction. Currently, the most comprehensive approach can be offered at centers with expertise in the management of acute complex airway disorders and availability of all endoscopic and surgical options.

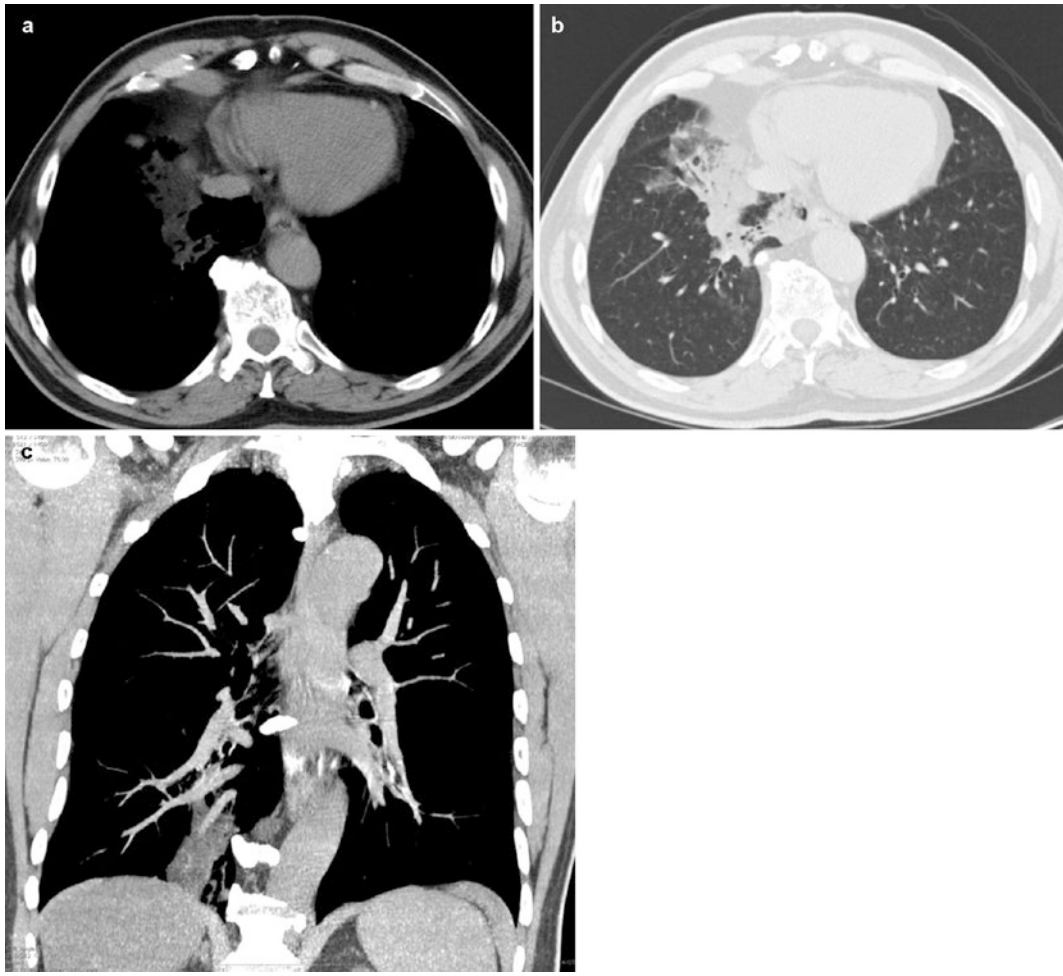

Fig. 11 Acute exogenous lipoid pneumonia. A 44-year-old actor performing in fire blowing shows who has aspirated liquid kindling for the grill 2 days before the onset of symptoms and was admitted acutely to the emergency department due to 38.8 °C fever, hemoptysis, pleuritic chest pain, and dyspnea. (**a**, **b**) Axial MDCT scans show a low-density consolidation in the middle lung lobe and scattered ground-glass opacities. (**c**) MDCT coronal MIP reconstruction better shows the low-density middle lobe consolidation. Region-of-interest measurements showed -60 to -80 Hounsfield units (HU), consistent with fat

2 Acute Exacerbation of Bronchiectasis

2.1 Introduction

The term bronchiectasis is derived from the Greek term *bronkia* (bronchial tubes), *ek* (out), and *tasis* (stretching), which together literally mean "the outstretching of the bronchi" (Feldman 2011). First described by Laennec in 1819, later detailed by Sir William Osler in the late 1800s, and further defined by Reid in the 1950s, this condition is generally defined as an abnormal and permanent focal or diffuse dilatation of the cartilage-containing airways (bronchi) caused by weakening or destruction of the muscular and elastic components of the bronchial walls (Hansell et al. 2008). Care must be taken to distinguish this large airway dilatation from dilatation of the small airways (bronchioles) that do not contain cartilage (Javidan-Nejad and Bhalla 2010). In contrast to established bronchiectasis

occurring in adults, some children with bronchiectasis have been shown to have resolution or considerable improvement of the changes seen on CT scanning, suggesting the possibility that the condition may be reversible in some cases (Al Subie and Fitzgerald 2010).

Bronchiectasis results from the occurrence of one of the three main pathogenic mechanisms: bronchial wall injury, bronchial lumen obstruction, and traction from adjacent fibrosis (Shoemark et al. 2007). The latter two mechanisms are usually apparent on imaging and are suggested by an endobronchial filling defect or adjacent interstitial lung disease, while when it is met the first mechanism the radiologist is faced with a more difficult differential diagnosis (Javidan-Nejad and Bhalla 2009). The dominant feature of bronchiectasis is clearly the presence of airway inflammation, in association with bacterial infection and, in particular, nonclearing infection. An initial airway insult, such as an infection, often on the background of genetic susceptibility, compromised host clearance mechanisms and, in particular, the mucociliary escalator mechanism, which facilitated persistent bacterial colonization and infection. This damages the airway further, both directly and indirectly, as a consequence of the initiation of a secondary host inflammatory response. The three pathogenic elements in bronchiectasis—namely, airway infection, inflammation, and enzymatic activities—interact to result in progressive airway damage. Many patients eventually harbor *Pseudomonas aeruginosa* (PA) in their airway, which is associated with significant morbidity (Pappalettera et al. 2009).

The Reid morphological classification, derived from bronchographic and autopsy studies, specifies three patterns (Reid 1950):

1. C*ylindrical or tubular* bronchiectasis in which there is relatively uniform dilatation of sections of the bronchial tree, involving diffuse mucosal edema, with resultant dilated bronchi but with straight, regular outlines and that end squarely and abruptly.
2. *Varicose* bronchiectasis in which there are local constrictions superimposed on cylindrical bronchiectasis (bulbous or beaded appearance), with alternating areas of dilatation and constriction and, potentially, obstructive scarring that may subsequently result in postobstructive pneumonia and additional parenchymal damage.
3. *Saccular or cystic* bronchiectasis in which there is progressive dilatation of the airways giving a balloon-like appearance and sometimes air–fluid levels; the number of bronchial divisions is greatly reduced; it is generally acknowledged that cystic bronchiectasis represents the most advanced disease (Fig. 12).

Oftentimes, more than one type of bronchiectasis can be seen in the same patient. As the airway dilatation increases, there may be progressive collapse and fibrosis of the distal lung parenchyma. Bronchiectasis can frequently occur in parallel with more common forms of chronic lung disease including COPD (up to 50 % of patients) and asthma (overlap syndromes) (Patel et al. 2004). There are many medical conditions that may lead to the development of bronchiectasis and these are detailed in Table 6.

2.2 Acute Exacerbations

The definition of an acute exacerbation is not standardized, and it has been variably defined to include some or all of the following symptoms and signs: increased cough and/or wheeze, sputum production/volume or purulence, dyspnea and lethargy, hemoptysis, or deterioration in spirometry (an unexplained significant, >10 %, reduction in FEV_1 or FVC over days or weeks), chest signs, and radiographic changes; especially in the presence of severe bronchiectasis, hypoxemia may also be present (Chang et al. 2008). Impaired clearance of secretions causes colonization and infection with pathogenic organisms, contributing to the purulent expectoration commonly observed in patients with acute exacerbation of bronchiectasis. The result is further bronchial damage and a vicious cycle of bronchial damage, bronchial dilation, impaired clearance of secretions, recurrent infection, and more bronchial damage (Cole 1984). *P. aeruginosa* often causes chronic bronchial infection in

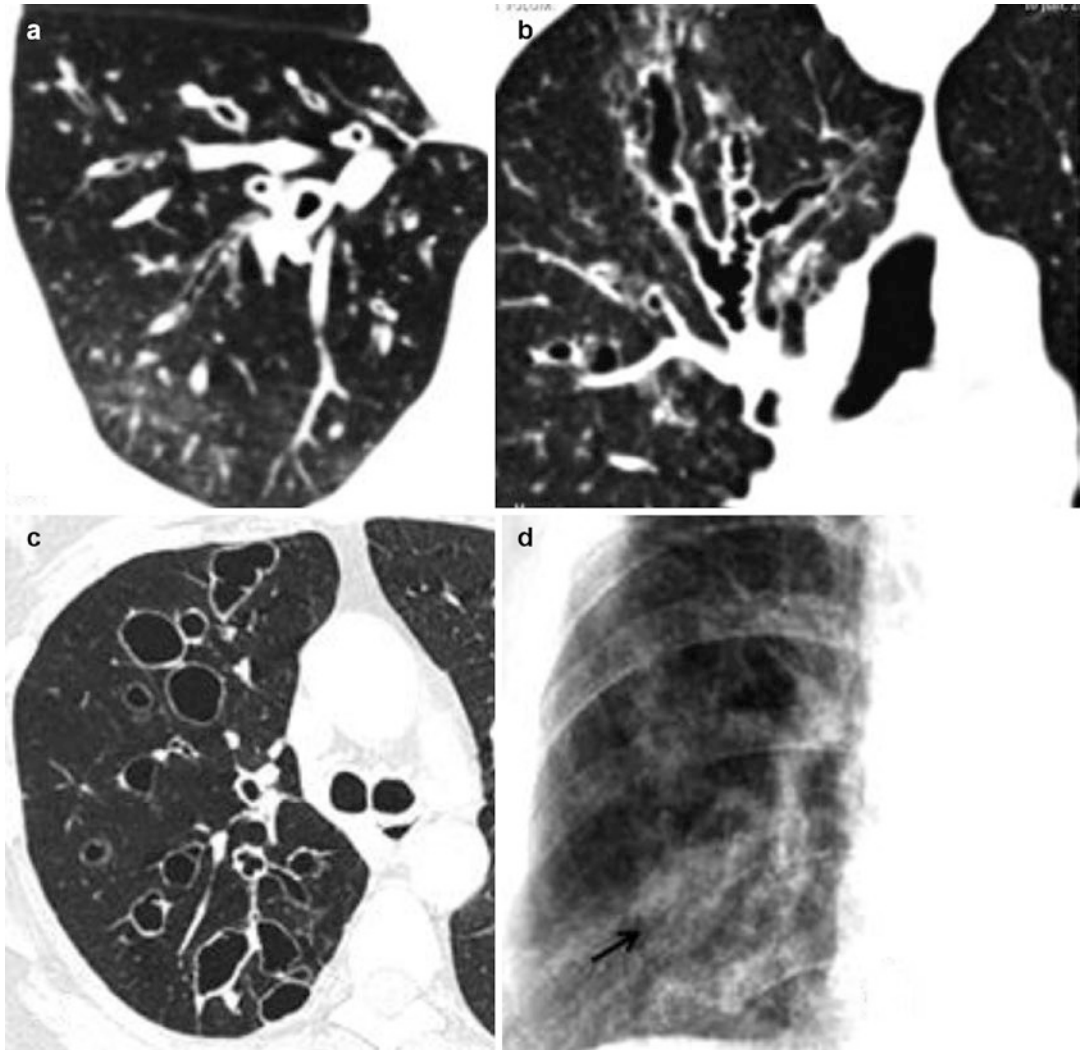

Fig. 12 The Reid morphological classification of bronchiectasis. (**a**) MDCT axial scan shows cylindrical or tubular bronchiectasis; (**b**) MDCT coronal reconstruction shows right upper lobe varicose bronchiectasis; (**c**) MDCT axial scan shows right upper lobe saccular or cystic bronchiectasis; (**d**) CXR close-up of the right lower lobe shows mucous plugging of bronchiectasis (*arrow*)

patients with non-CF bronchiectasis via a mechanism involving biofilm formation and the release of virulence factors. This suggests that *Pseudomonas* species may promote disease progression and that infection with these species may be related to worsening lung function and increased morbidity and mortality (Davies et al. 2006). Patients with chronic obstructive pulmonary disease are prone to prolonged exacerbations. Although hemoptysis is common during infective exacerbations of bronchiectasis, it may also occur in the absence of concurrent infection, so-called *dry bronchiectasis*, which is usually a sequela of tuberculosis and is found in the upper lobes. Hemoptysis, sometimes life-threatening, is caused by chronic airway inflammation and hypoxemia, which leads to bronchial arterial neovascularization (Bruzzi et al. 2006). Finally, acute exacerbations of bronchiectasis are associated with increased mortality, and the

Table 6 Causes of bronchiectasis

Causes of bronchiectasis	Imaging findings to provide clues to the diagnosis
Idiopathic (48%)	*Often a lower lobe distribution*
Post-infective (25%)	
Severe pneumonia	
Tuberculosis	
NTM	*Prominent nodularity in a tree-in-bud pattern or with cavitation*
Pertussis	*Lower lobe predominance*
Measles	
Impaired mucociliary clearance (9%)	
CF	*Bilateral, proximal, parahilar, predominantly upper lobe disease*
Primary ciliary dyskinesia	*50% associated with situs inversus, middle lobe/ lingular predominance*
Young's syndrome	*Predominantly lower lobe disease*
Chronic obstructive pulmonary disease and smoking	
Immunodeficiency (8%)	
Common variable immunodeficiency	
Hypogammaglobulinemia	*Disproportionate bronchial wall thickening*
Specific polysaccharide antibody deficiency	
Secondary immunodeficiency, e.g., malignancy (chronic lymphocytic leukemia)	
Human immunodeficiency virus infection	
Lung and bone transplantation	
Exaggerated immune response	
Allergic bronchopulmonary aspergillosis	*Upper lobes, central bronchiectasis, prominent mucus plugging*
Graft versus host disease	
Inflammatory bowel disease (ulcerative colitis and Crohn's disease)	
c-ANCA-positive vasculitis	
Rheumatoid arthritis (3.2–35% of patients)	
Congenital abnormalities of the bronchial wall	
Mounier-Kuhn syndrome	(*tracheobronchomegaly; enlarged tracheal diameter:>25 mm men, >23 mm women; trachea and bronchi of first to fourth order; central bronchiectasis)*
Williams-Campbell syndrome	(congenital absence of cartilage from lobar to first- to second-generation segmental airways)
Marfan syndrome	
Job syndrome (hyperimmunoglobulin E syndrome)	
Inflammatory pneumonitis	
Aspiration of gastric contents	
Inhalational exposure (smoke, ammonia, chlorine)	
Fibrosis (traction bronchiectasis)	
Sarcoidosis, radiation fibrosis, end-stage HP	*Predominantly upper lobes disease*
Idiopathic pulmonary fibrosis	*Predominantly lower lobes disease*
Mechanical obstruction (postobstructive)	*Unilateral focal bronchiectasis*
Foreign body	
Tumor	
Extrinsic compression (e.g., lymph node)	

(continued)

Table 6 (continued)

Causes of bronchiectasis	Imaging findings to provide clues to the diagnosis
Miscellaneous conditions	
Primary *Mycobacterium avium complex*	*Classic subtype: tree-in-bud opacity, patchy consolidation/cavities, upper lobes and superior segments of lower lobes*
"Lady Windermere syndrome"	*Nonclassic subtype: predominantly middle lobe and lingular disease*
Connective tissue diseases (e.g., rheumatoid arthritis, systemic lupus erythematosus, Sjogren's syndrome)	
Pulmonary sequestration	
Yellow nail syndrome	
Infertility (primary ciliary dyskinesia, cystic fibrosis, Young syndrome)	
Diffuse panbronchiolitis	
a1-Antitrypsin deficiency	
Smoke and gaseous toxins (e.g., chlorine gas and ammonia)	

majority of deaths are related to respiratory infection, with higher mortality rates associated with increasing age and number of lobes affected.

2.3 Clinical and Imaging Diagnosis

The diagnosis of bronchiectasis should be suspected in any individual presenting with persistent daily cough with mucopurulent sputum, recurrent hemoptyses, frequent infective exacerbations, and finger clubbing (Boyton 2012). The severity of airflow limitation is related to the extent and severity of the bronchiectasis (Javidan-Nejad and Bhalla 2009). In approximately 50% of patients, a specific cause of bronchiectasis is not determined; however, in a substantial percentage of adult and children, the finding of an underlying cause results in a change in therapy and may have significant prognostic implications. The lung function studies in patients with bronchiectasis usually show an obstructive defect, and there may or may not be evidence of airway hyperreactivity. In all newly diagnosed patients with bronchiectasis, sputum should be cultured for bacteria and mycobacteria, and fungal cultures could be considered in selected cases. The main bacterial pathogens that are commonly isolated are *Haemophilus influenzae* (29–70%) followed by *Pseudomonas aeruginosa* (12–31%). Imaging now forms the cornerstone of diagnosis of bronchiectasis and its complications and plays an increasing role in disease monitoring and therapeutic planning.

2.3.1 Chest Radiography (CXR)

A plain chest radiography (CXR) is useful as an initial screening tool and, during acute exacerbations, may raise the initial suspicion of bronchiectasis, triggering more definitive imaging. However, it is insufficiently sensitive for the adequate diagnosis of the condition (sensitivity<50%) (Goeminne and Dupont 2010; Currie et al. 1987), particularly in mild disease (Table 7).

Despite the obvious CXR deficiencies for the identification of bronchiectasis, an appreciation of the sometimes subtle radiographic features is necessary (Fig. 13) (Gudbjerg 1955; Woodring 1994):

(a) With more severe bronchial inflammation and fibrosis, the bronchial walls themselves become visible as parallel lines (*tram lines* or *tram tracks*) most obvious in the lower lobes on a PA view and in the middle lobe or lingula on the LL view (Westcott 1991; Feldman 2011) (Fig. 13).

Table 7 Bronchiectasis: CXR direct and indirect findings

Direct signs	Indirect signs
1. *Parallel line opacities* (*tram lines* or *tram tracks*) by dilated, thickened bronchi seen along their length	1. *Indistinct margins of vessels*
2. *Ring opacities* or *cystic* spaces (as large as 2 cm in diameter) when the bronchus is seen on end or from cystic bronchiectasis, sometimes with *air–fluid levels* (demilunes)	2. *Volume change*
3. *The signet ring sign*	(a) *Volume loss*
4. *Tubular and ovoid opacities* as *Y* or *V* shapes and sometimes the appearance of a *gloved finger* or as "finger-in-glove" opacities which radiate from the pulmonary hilum, from mucus plugging	Obscuration of the underlying hemidiaphragm
5. *Other signs:* scarring, bulla formation, pleural thickening	Crowding of pulmonary vascular markings Fissural displacement
	(b) Overall lung *volume increased* (compensatory hyperinflation and in generalized bronchiectasis such as in CF)
	3. Areas of *consolidation* (may be due to infection) (e.g., *Pseudomonas aeruginosa* or in ABPA)

(b) When seen end on, bronchiectatic airways appear as *ill-defined ring shadows*, ranging in size from 5 to 20 mm, notably in the mid and upper zones where the majority of airways run parallel to the radiograph beam. Signs of complications/exacerbations, such as dilated bronchi filled with pus and mucus, result in *tubular and ovoid opacities* and sometimes in the dramatic appearance of a *gloved finger*, typically seen in patients with mucoid impaction of the airways due to allergic bronchopulmonary aspergillosis (ABPA) (Fig. 14) (Martinez et al. 2008).

(c) In severe cystic disease, multiple *thin-walled ring shadows* that may contain *fluid levels* are present; the *signet ring sign* corresponds to a dilated bronchus immediately adjacent to a smaller companion pulmonary artery (Hansell 1998).

(d) Because the bronchi lie alongside the pulmonary arteries, peribronchial inflammation in early bronchiectasis makes the *margins of vessels indistinct*, particularly in the lower lobes (Hansell 1998).

(e) Associated volume loss in the lower lobes may cause *obscuration of the underlying hemidiaphragm* and *crowding of pulmonary vascular markings*, usually caused by mucous obstruction of the peripheral bronchi (Westcott 1991).

(f) Additional features of focal areas of *subsegmental collapse* and *patchy peribronchial consolidation* are nonspecific but are common in generalized disease.

(g) Signs of compensatory hyperinflation of the unaffected lung (Hansell 1998).

Extensive parenchymal consolidation is not, contrary to what might be expected, a usual feature of an infective exacerbation of bronchiectasis. Repeated infective exacerbations of subpleural bronchiectatic airways may result in a pleural reaction, although extensive pleural disease is rare unless there has been an associated empyema.

2.3.2 Thin-Section CT

Bronchography was replaced many years ago by high-resolution CT (HRCT) scanning of the chest (Young et al. 1991), which has become the gold standard (the most sensitive and specific noninvasive method, respectively, 84–97 % and 82–99 %, but higher at referral centers) for the diagnosis and that contrasts starkly with the limited ability of CXR to detect even advanced bronchiectasis (Hansell 1998). The detail afforded by 1-mm images of the peripheral airways has proved superior to virtually every other method for assessing the extent and severity of disease. Furthermore, thin-section CT features may be

Fig. 13 Chest radiography findings in bronchiectasis. (**a**) In both upper lobes, CXR shows parallel tubular opacities due to partial fluid-filled airways. (**b**) The signet ring sign (*arrow*), a dilated bronchus immediately adjacent to a smaller companion pulmonary artery. (**c**, **d**) Integrated imaging (CXR and MDCT) shows upper right lobe ring opacities or cystic spaces, sometimes with air–fluid levels (demilunes)

suggestive of certain underlying conditions but require correlation with clinical and laboratory assessments, and images should be examined for findings suggesting ABPA, cystic fibrosis, immotile cilia, opportunist mycobacteria, and tracheobronchomegaly (Fig. 15) (Milliron et al. 2015).

Multidetector CT (MDCT) with volumetric acquisition, subsecond data acquisition, and initial thinnest possible collimation minimizes respiratory and cardiac motion, allows isotropic image reconstructions, and increases the sensitivity in detection of subtle nontapering airways, opening potentially unique automated, quantitative methods for evaluating the peripheral airways (Studler et al. 2005; Sung et al. 2003). Using MDCT as the gold standard, the sensitivity, specificity, and positive and negative predictive values of incremental HRCT in detecting bronchiectasis were 71 %, 93 %, 88 %, and 81 %, respectively (Hill et al. 2010; Dodd et al. 2006).

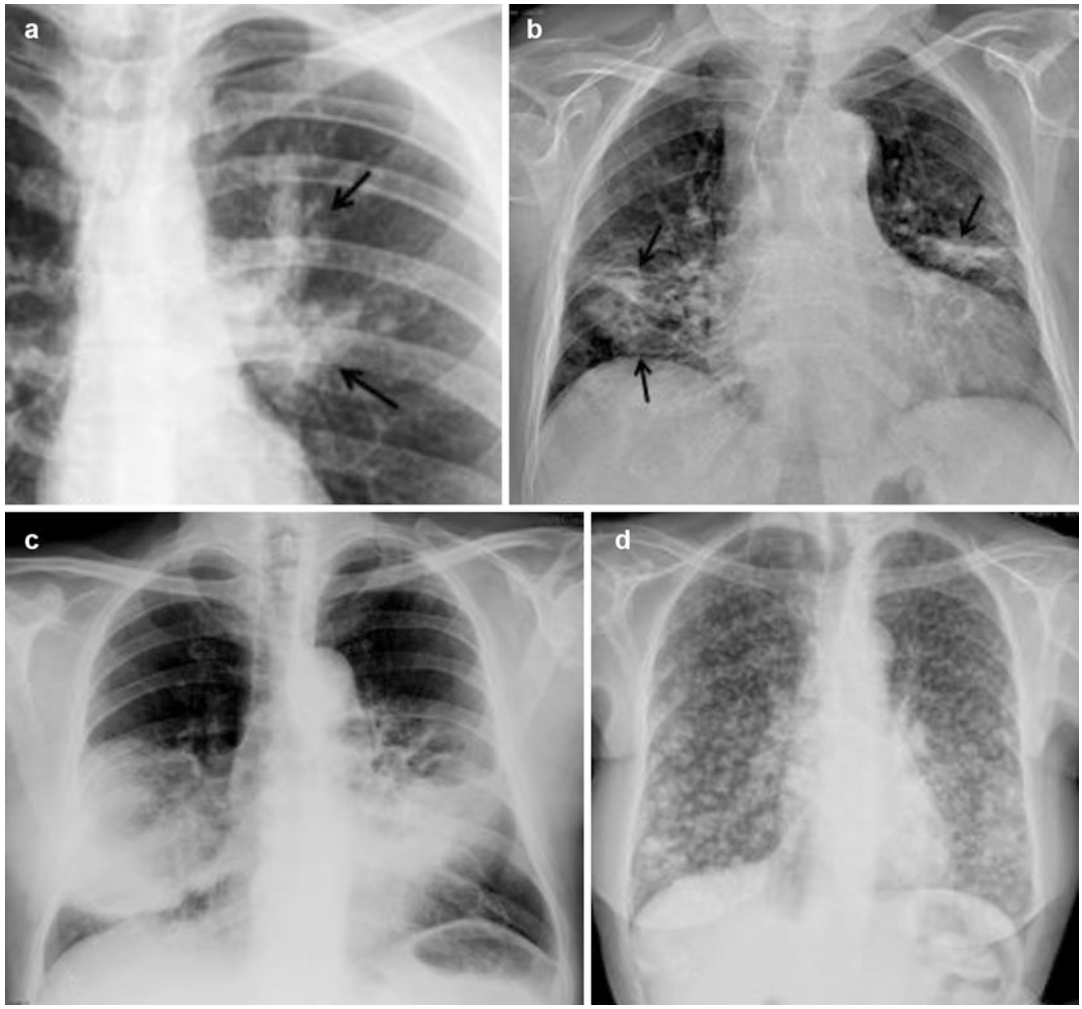

Fig. 14 Chest radiography findings in acute exacerbation of bronchiectasis. (**a**) CXR of a parahilar "gloved finger," typically seen in patients with mucoid impaction of the airways due to ABPA (*arrows*). (**b**) Bilateral focal areas of subsegmental collapse and patchy peribronchial consolidation from mucous plugging (*arrows*). (**c**) Large consolidations in both mid-lower lungs are an unusual feature of an infective exacerbation of bronchiectasis. (**d**) CXR shows diffuse lung nodular-like pattern from mucous filled airways (*P. aeruginosa*)

Interobserver agreement for the presence, extent, and severity of bronchiectasis was also better for MDCT (kappa 0.64, 0.5, and 0.48, respectively) than for incremental HRCT (kappa 0.65, 046, and 0.25, respectively) (Dodd et al. 2006). Because today most patients present with relatively mild bronchiectasis, with few (if any) physical signs, the diagnosis is usually made by *a combination of the patient's history and a thin-slice MDCT examination.* It is important to include expiratory imaging as part of the routine MDCT acquisition (Bankier et al. 1996). If it is possible, continuous acquisition of images during a forced or slow expiratory maneuver (dynamic expiratory CT) is not only more sensitive for detection of air trapping but also leads to identification of air trapping in normal individuals (Gotway et al. 2000). MinIP reconstructions are useful to demonstrate winding, interconnected tubular structures. Serious limitations for the use of quantitative airway measurements, most often including lumen diameter,

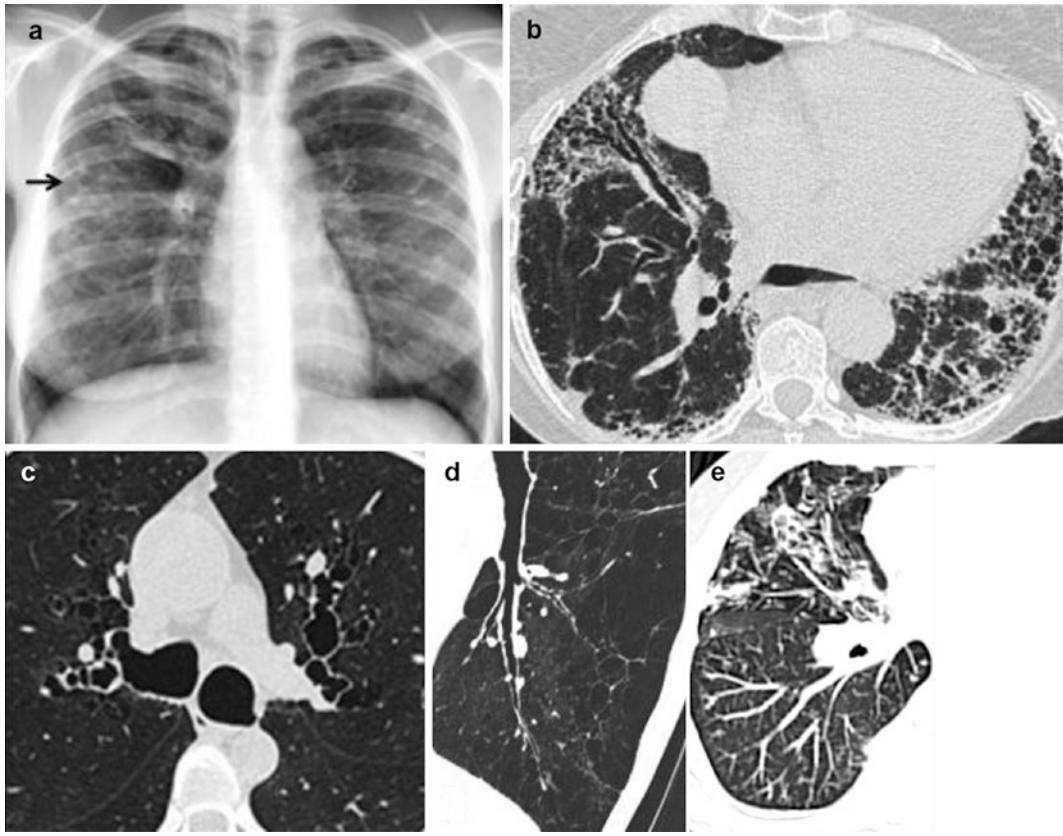

Fig. 15 Imaging findings suggestive of related diseases in bronchiectasis. (**a**) In cystic fibrosis (CF), CXR findings include hyperinflation, mucoid impactions, and bilateral parahilar mainly upper lobe bronchiectasis (*arrow*). (**b**) Traction bronchiectasis in fibrotic idiopathic interstitial pneumonia caused by peribronchial scarring. (**c**) Mounier-Kuhn syndrome is an idiopathic disease secondary to a marked atrophy of the elastic fibers and smooth muscle within the wall of the trachea and main bronchi; MDCT axial scan shows enlargement of the lumen in inspiration (>3 cm) and collapse during expiration (not shown). (**d**) Bronchiectatic airway remodeling in COPD. (**e**) ABPA bronchiectasis: ABPA is a hypersensitivity reaction to Aspergillus fumigatus antigens, affecting mostly patients with asthma and cystic fibrosis; bronchiectasis, mainly centric and in the upper lobes, is the hallmark of the disease. In ABPA retained secretions may appear sufficiently dense to mimic calcification or may calcificate

bronchoarterial ratio (BAR), lumen area (LA) and volume, wall thickness/diameter ratio (T/D ratio), and wall area percent (WA%), have been repeatedly documented, and none of these have proved of value in everyday routine clinical practice (Brillet et al. 2009; Williamson et al. 2009). As a consequence of these limitations, visual inspection remains the standard for clinical assessment of airway disorders; the potential for new methods for obtaining clinically useful automated quantitative airway evaluation remains to be evaluated. The extent of involvement of the lungs documented on HRCT scanning has been shown to correlate with both functional changes (PFT) and clinical outcomes, and HRCT score correlates significantly with exacerbation frequency (Brody et al. 2005). Although volumetric CT has numerous advantages, the radiation dose is higher and can be mitigated by several techniques (McCollough et al. 2009). Because of concerns of the level of radiation exposure with CT, particularly in children, MRI has been

studied more recently for the diagnosis of bronchiectasis and been found to be a potentially suitable radiation-free alternative to CT, although the poorer spatial resolution of MRI limits the ability to visualize smaller airways and nodules (Montella et al. 2009). The most specific thin-slice CT scanning direct findings suggestive of bronchiectasis are (Table 8) (Naidich et al. 1982; Grenier et al. 1986; Hansell 1998; Javidan-Nejad and Bhalla 2009; King and Daviskas 2010; Bonavita and Naidich 2012) (Fig. 16):

1. Bronchoarterial ratio (BAR) > of 1–1.5: internal diameter of the bronchus is wider than the adjacent pulmonary artery at an equivalent branching level (i.e., a dilated bronchus cut in a horizontal section with an adjacent pulmonary artery representing the stone, signet ring formation); severity can be graded as mild, moderate, or severe (luminal diameter slightly greater, 2–3 times or >3 times than that of adjacent blood vessel in Bhalla scoring system). Care must be taken not to misinterpret bronchial dilatation as bronchiectasis in the setting of underlying acute parenchymal consolidation (so-called reversible bronchiectasis).
2. Failure of the bronchi to taper (bronchial diameter should remain unchanged for at least 2 cm distal to a branching point), a finding best appreciated toward the outer one-third of the lungs; however, this sign can be difficult to interpret in nonvolumetric CT studies (Kim et al. 1997a, b).
3. The bronchi being visualized in the outer 1–2 cm of the lung fields and visibility of airways within 1 cm of the pleural surface or abutting the mediastinal pleural surface (Kim et al. 1997a, b). Mucus plugging of dilated bronchi is readily identified, causing either complete or partial luminal filling and may be reversible. Plugging of the smaller peripheral airways and peribronchiolar inflammation are characterized by a tree-in-bud appearance, with V- and Y-shaped branching nodular opacities (Fig. 17).

Table 8 Bronchiectasis: thin-section CT direct and indirect findings

Direct signs	Indirect signs
1. *Bronchial dilatation*	1. *Bronchial wall thickening*
Increased bronchoarterial ratio (BAR)	Best assessed visually on images obtained at right angles through vertically oriented airways
Contour abnormalities (wall thickening)	2. *Mucoid impaction/ fluid-filled airways*
2. *Lack of airway tapering* >2 cm distal to point of bifurcation	Tubular or Y-shaped structures; branching or rounded opacities in cross section +/– air–fluid levels
3. *Airway visibility within 1 cm* of the costal pleura or fissures	3. *Bronchiolitis* Clustered ill-defined centrilobular nodules with a tree-in-bud configuration 4. *Mosaic attenuation caused by air trapping* Best identified on expiratory HRCT images 5. *Mosaic perfusion* Better identified on contrast-enhanced dual-energy CT of the pulmonary parenchyma 6. *Bronchial artery hyperplasia* 7. *Pulmonary hypertension findings*

The severity of bronchiectasis can also be assessed on the basis of the extent of disease, mucous plugging, and sacculations or abscesses and in terms of the number of bronchial divisions and lobes/segments involved, and a radiographic severity scoring system developed for use in CF has been used to assess patients with non-CF bronchiectasis (Bhalla et al. 1991). *Mosaic attenuation* is a term used to denote heterogeneous lung density, often exhibiting a distinctly geographic distribution. This nonspecific finding typically results from one of the following three causes: (1) foci of abnormally increased lung density caused by a variety of infiltrative and/or airspace filling diseases; (2) alternating low-density and high-density foci reflecting variations

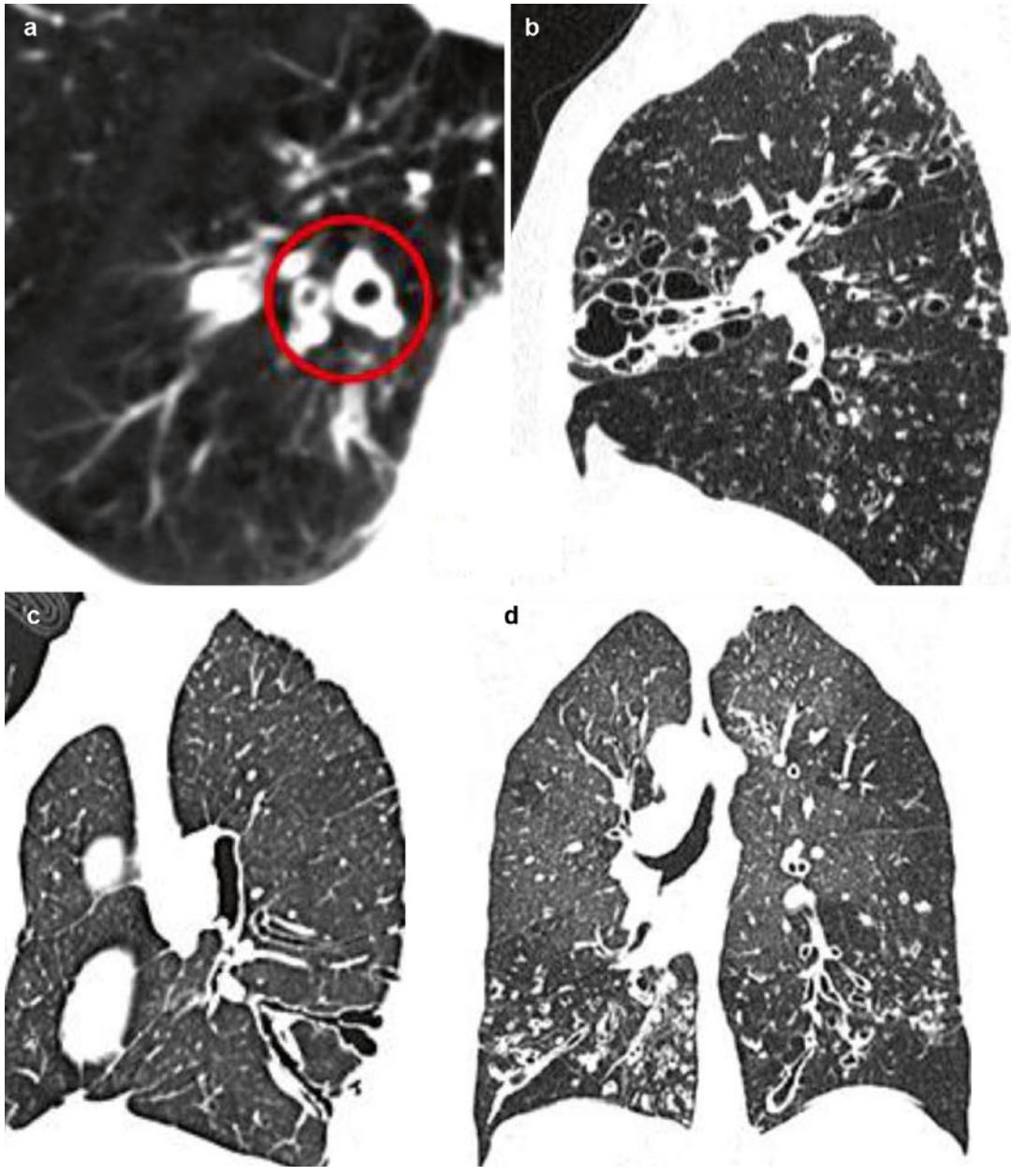

Fig. 16 Thin-section CT findings in bronchiectasis. (**a**) The so-called signet ring sign (*circle*), a bronchus with an internal diameter greater than the diameter of the adjacent pulmonary artery. (**b**) Sagittal reconstruction shows a bronchiectatic bunch of grapes in the middle lobe. (**c**) Sagittal reconstruction shows lack of airway tapering >2 cm distal to point of bifurcation, bronchial wall thickening, and bronchi abutting the pleural surface. The wall thickness evaluation varies depending on slice thickness and window levels. (**d**) Coronal reconstruction shows lack of airway tapering and mosaic attenuation pattern

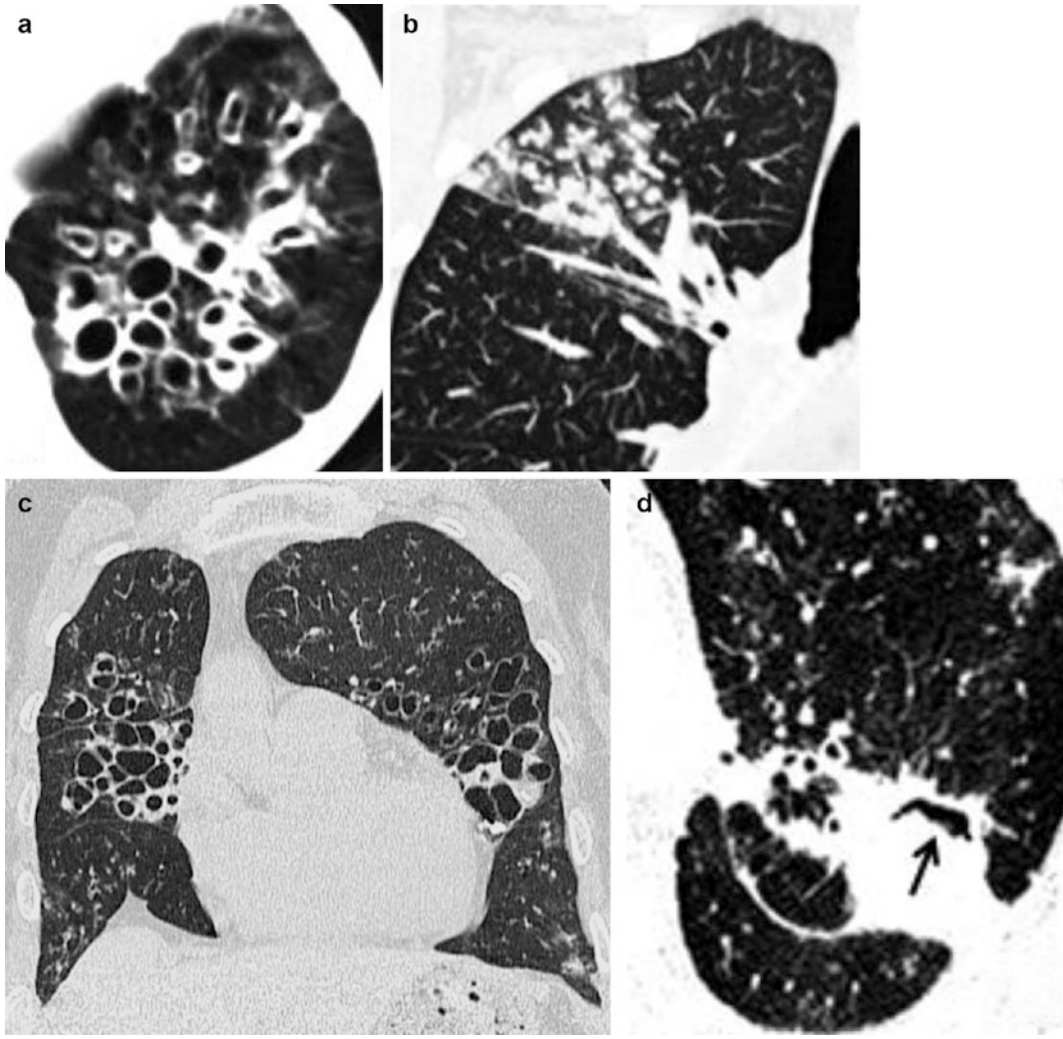

Fig. 17 Computed tomography findings in acute exacerbation of bronchiectasis. (**a**) Axial scan shows ring clustered cystic spaces in the lower right lobe with air–fluid levels (demilunes). (**b**) Coronal reconstruction shows right upper lobe clustered ill-defined centrilobular nodules with a tree-in-bud configuration by mucus-impacted small airways (bronchiolitis). (**c**) Coronal reconstruction shows bilateral cystic exacerbated bronchiectasis with air–fluid levels. (**d**) Axial closeup scan shows cystic bronchiectasis with fungal overinfection/mycetoma (*arrow*)

in lung perfusion, characteristically the result of chronic embolic pulmonary hypertension; and (3) foci of abnormally decreased lung density caused by focal air trapping in patients with underlying obstructive small airway disease (Bonavita and Naidich 2012). Differentiation between these causes is best accomplished on images acquired in deep expiration. Air trapping results either from mucous plugging and abnormal bronchial compliance or inflammation/fibrosis of the small airways, reflecting a combination of both large and small airway obstruction.

Another ancillary finding is the *presence of dilated bronchial arteries* in patients with long-standing severe bronchiectasis. This finding is easily identified following administration of intravenous contrast as irregular, tortuous vessels arising from the proximal descending thoracic

aorta extending along the central airways toward the pulmonary hila. Identification of hypertrophied bronchial arteries may explain hemoptysis that is otherwise unaccounted for in select acute exacerbation cases (Fig. 18).

In acute exacerbation, more frequent imaging findings are air–fluid levels in bronchiectatic airways, mucous plugging, centrilobular nodules, and peribronchial thickening, all potentially reversible signs.

A variety of different CT-based methods for assessing the *extent and severity* of disease have been proposed (Bhalla et al. 1991; Ooi et al. 2002; de Jong et al. 2004; Oikonomou

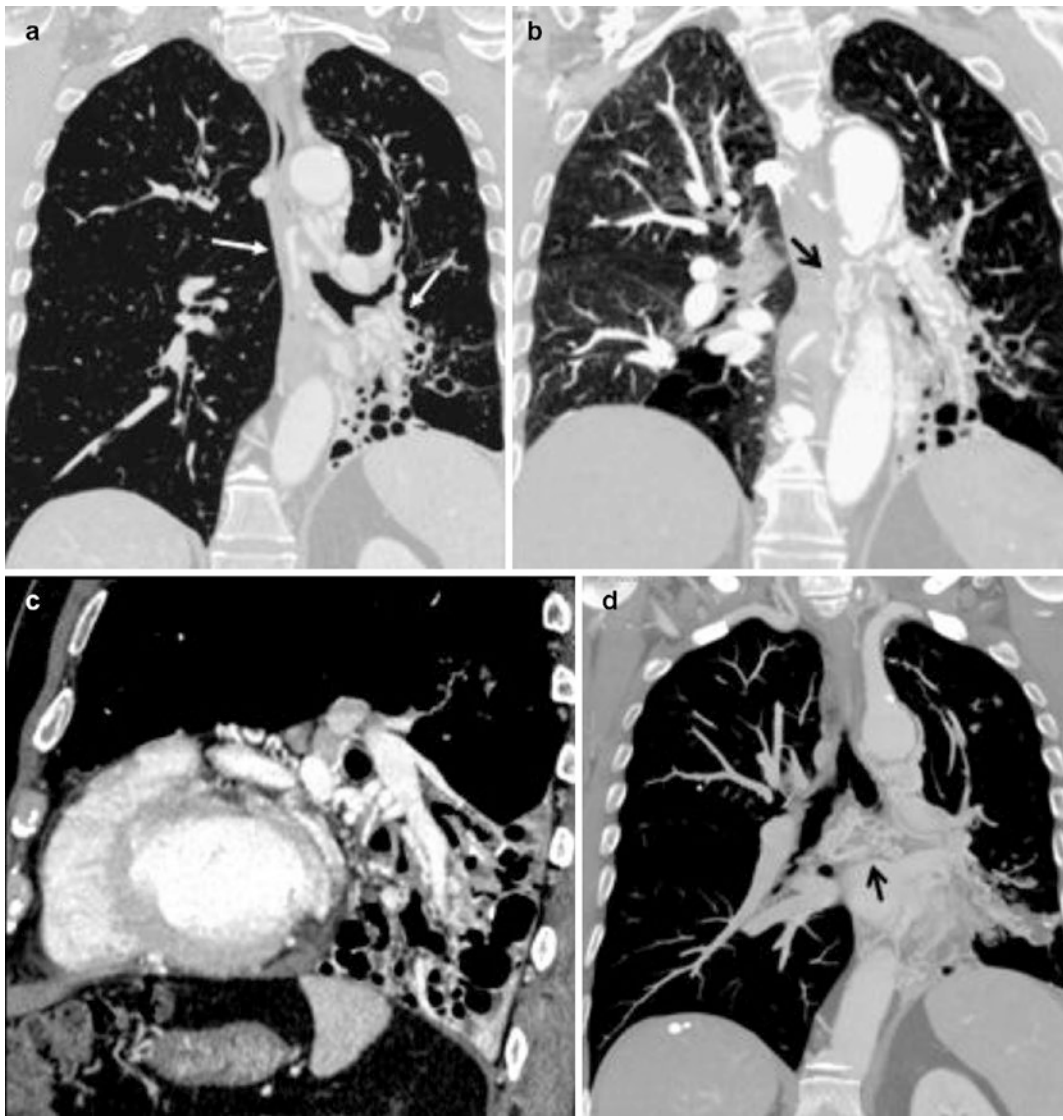

Fig. 18 Massive hemoptysis in a 41-year-old man with common variable immunodeficiency and a history of recurrent infections beginning during childhood. MDCT arterial phase (**a**, **b**, **d**) coronal and (**c**) oblique sagittal reconstructions reveal bilateral lower lobes bronchiectasis with mosaic attenuation and focal consolidation (likely hemorrhage) and tortuous hypertrophied bronchial arteries (*arrows*). The patient was treated with repeated bronchial artery embolizations

et al. 2008); they have emphasized a few or all of the following: generations of bronchial divisions (including the number of lobes/segments involved), peribronchial thickening, mucoid impaction (both large and small airway, the latter identified as resulting in a tree-in-bud pattern), signs of obstructive airway disease including CT evidence of emphysema, and mosaic attenuation (especially as documented on expiratory images). Although clearly requiring further validation, it is apparent that true routine, automated, quantitative global scoring of bronchiectasis (including color-coded 3D maps and dual-energy CT measurements of airway wall enhancement) is feasible and, if established (Bonavita and Naidich 2012), would represent an important milestone in the use of CT to assess patients with a wide variety of airway diseases.

2.4 Summary

Imaging plays a crucial role in the diagnosis and monitoring of bronchiectasis and the management of complications. CXR is useful as an initial screening tool and during acute exacerbations, but has limited sensitivity and specificity. Thin-section MDCT is the reference standard for diagnosis, quantification, and low-dose routine surveillance of bronchiectasis, providing detailed morphological and physiologic consequence evaluation; furthermore, it is valuable in diagnosing and managing complications in exacerbations and acute setting.

3 Toxic Gas Inhalation

3.1 Introduction

Acute injury to the airways and lung parenchyma may occur as a result of an industrial disaster, occupational exposure, recreational mishap, natural catastrophe, chemical warfare, and acts of terrorism (Kales and Christiani 2004). According to AEGL, acute exposures are single, non-repetitive exposures that do not exceed 8 h (Acute Exposure Guideline Levels, AEGLs).

In industrialized countries, most acute toxic inhalations come from industries, home, and recreational sources; new industrial practices and materials are increasingly recognized as causes of acute lung disease, but much of our present knowledge of inhalation injury has been gathered from burn units in smoke inhalation injury (SII), where pulmonary insufficiency is a major cause of death (Rabinowitz and Siegel 2002). In this section, we illustrate the spectrum at imaging of lung injury related to acute toxic exposures.

3.2 Definitions and Classification

Numerous classification schemes have been developed as a way to organize the enormous numbers of possible inhaled toxicants (Table 9) (Rabinowitz and Siegel 2002; Miller and Chang 2003; Nelson and Hoffman 2006; McKay 2014; Borron and Bebarta 2015; Salem and Katz 2015).

Table 9 Scheme of possible inhaled toxicants

Gases	A state of matter consisting of particles that have neither a defined volume nor a defined shape at normal temperatures and pressures and can expand to occupy an available space
Vapors	A condensable gas, that is, a state of matter that can be converted to another physical form by alterations of temperature and/or pressure, but there are no significant chemical or physical differences between a vapor and a gas
Fumes	They form when a solid, which has been volatilized by evaporation or vaporization, condenses in cool air
Particulates	Microscopic solid or liquid matter suspended in a medium, usually air in the Earth's atmosphere
Aerosols	Commonly refers to the particulate/air mixture, as opposed to the particulate matter alone
Dusts	Suspensions of solid particles in a gaseous media
Smokes	Result from the incomplete combustion of carbon-containing material including oil and coal

The severity pattern of disease is a function of the toxin or mix of toxins (*particle size*, *density*, *water solubility*, *shape*) that constituted the exposure, *duration* of *exposure*, *minute ventilation*, and the host factor status of the individual. The total inhaled dose is equal to agent concentration multiplied by time of exposure and minute ventilation (Rabinowitz and Siegel 2002; Borron and Bebarta 2015; Nelson and Hoffman 2006; McKay 2014; Salem and Katz 2015). The effects of inhalation exposure to toxicants can be thought of as follows: simple asphyxiants, tissue asphyxiants, nonrespiratory systemic toxicants with pulmonary absorption, and direct airway cellular injury. Such injuries in general occur either through localized pulmonary damage or by systemic absorption after inhalation (Miller and Chang 2003).

Those that cause localized pulmonary damage can be subdivided further into *irritant gases* (in that the chemical interaction of the agent and the water at the mucosal surface of the airways and/or other cellular components results in direct tissue injury via the generation of acids, alkali, or other reactive compounds) and those that cause *pulmonary sensitization* (associated with the late occurrence of "reactive airway dysfunction syndrome" or RADS in which subsequent exposure to small concentrations of the same agent or other potential respiratory irritants results in an asthma-like condition with bronchospasm, bronchoconstriction, and decreased airflow; RADS is not associated with immunoglobulin E-mediated histamine release) (Gorguner et al. 2004). Those that cause systemic toxicity can be subdivided into *simple asphyxiants* (displace atmospheric oxygen following Dalton's law of partial pressures but are otherwise essentially physiologically inert), *systemic asphyxiants* (usually interfere with transport or use of oxygen within tissues and organs; some chemicals exert systemic toxic effects when absorbed by way of the pulmonary circulation but cause no direct acute airway or lung injury), *organophosphates*, *hydrocarbons,* and *metal fumes* (Table 10) (Rabinowitz and Siegel 2002; Mokhlesi and Corbridge 2003; Borron and Bebarta 2015; Salem and Katz 2015).

Table 10 Pulmonary and systemic main inhalational toxicants

Pulmonary inhalational toxicants	Systemic inhalational toxicants
Irritant gases	*Asphyxiants*
Ammonia	Carbon monoxide (CO)
Chlorine	Methemoglobin inducers[a]
Formaldehyde	Hydrogen cyanide (HCN)
Nitrogen dioxide	Hydrogen sulfide (H2S)
Phosgene	Carbon dioxide (CO_2)
Hydrogen fluoride	Nitric oxide (NO)
Acrolein	Methane
Ozone	Helium, argon, krypton, xenon
Antigens/sensitizers	*Organophosphates*
Ammonia	Nerve gases (cholinesterase inhibitors)
Chlorine	Sarin (GB)
Formaldehyde	Tabun (GA)
Nitrogen dioxide	Soman (GD)
Methyl isocyanate (MIC)	Venon X
Toluene	Insecticides
Vinyl plastics	*Hydrocarbons*
Animal and plants proteins	Freon
Bacteria	Benzene
Fungi	Toluene
	Vinyl chloride
	Trichloroethylene
	Trichloroethane
	Metal fumes
	Beryllium
	Cadmium
	Mercury
	Nickel
	Zinc
	Chromium

There can be significant overlap, as many toxicants can fit in multiple categories

[a]Methemoglobinemia is a state of oxidized hemoglobin in which the hemoglobin iron is in the ferric state (Fe^{31}) and is unable to bind to or transport oxygen

3.3 Mechanisms of Toxicity

Direct airway cellular injury results from epithelial cell injury and death and from airway edema; the *nasopharynx* and *larynx* manifest these cellular injuries earliest because they are exposed to the highest concentrations of inhaled toxicants

(Garnier 1998; Mokhlesi and Corbridge 2003). Gases that are *highly water-soluble*, such as ammonia, sulfur dioxide, and hydrogen chloride, generally cause acute irritant injury to mucus membranes, including the eyes and the lining of the nose and upper airway, and spare the lower respiratory tract. This irritant injury causes unpleasant symptoms that often encourage an individual to rapidly leave an area of exposure; this prevents more severe clinical effects. *Less soluble gases*, such as phosgene, ozone, and nitrogen oxides, often cause no symptoms or ill effects in the upper airway. They penetrate into the lower airway and cause irritant effects in the bronchi, terminal bronchioles, and alveoli. Pulmonary irritants with *intermediate solubility* can produce a mixed clinical picture; whether upper or lower tract symptoms predominate depends on the duration and intensity of the exposure. Chlorine gas is a prototypical example of an intermediate solubility irritant and can produce a broad spectrum of clinical syndromes depending on the circumstances surrounding a given exposure (Rabinowitz and Siegel 2002). There is a gradual but progressive airway response to direct cellular injury. Within a few hours of postexposure, there is extensive but mild mucosal edema, no ulceration, and deceptively minimal clinical symptoms. Over the next 8–48 h, there is progressive airway edema, mucopurulent membrane production, and bronchorrhea. Within 48–72 h, there is mucosal slough and evolution of a membranous tracheobronchitis.

If toxic agents pass to the level of the *conducting airways*, damage to the epithelial cells and tight junctions can increase mucosal permeability to other substances, which increases inflammation and cellular damage. This can lead to bronchoconstriction, peribronchial edema, and bronchial mucosal slough and all can contribute to the development of atelectasis. Substances that have lower water solubility and particles less than 5 μm in diameter can penetrate into the lower respiratory tract. In the *distal airways and alveoli*, epithelial and endothelial injury results in permeability-induced edema. This can manifest anywhere from mild interstitial edema to pulmonary insufficiency. As in other forms of the acute respiratory distress syndrome (ARDS), this results in decreased lung compliance, increased alveolar-arterial oxygen gradient, and increased pulmonary vascular resistance (Ferguson et al. 2012; Fanelli et al. 2013). Pulmonary edema may be immediate in pulmonary high-concentration toxicant exposure or may be delayed 24–48 h postexposure (Miller and Chang 2003). Aggressive supportive care is often lifesaving, and treatment is usually symptomatic with the exception of organophosphates, certain chemical asphyxiants, such as cyanide and carbon monoxide, and opioid poisonings and toxicant-induced methemoglobinemia (Endorf and Gamelli 2007; Micak et al. 2007; Heitkamp et al. 2012). Airway injury is present in up to one-third of patients with major burns. Pulmonary insufficiency is a major cause of death in burn victims from residential or commercial structure fires and has been shown to result from inhalation of toxic products of combustion including the oxides of sulfur, nitrogen, aldehyde gases, and particulates, rather than from thermal injury. Carbon monoxide is rapidly transported across the alveolar membrane and binds to hemoglobin. Smoke inhalation also adds to mortality from cutaneous thermal burns and represents a combination of direct pulmonary injury and systemic and metabolic toxicities (mortality rates are approximately 5–8 %) (Table 11) (Darling et al. 1996).

Table 11 Factors of lung pathophysiologic response to smoke inhalation injury (SII)

Smoke lung injury
Patient preinjury health status (reactive airway disease or chronic lung changes)
Direct mucosal injury compromises the mucociliary escalator and particulate, mucus, and bacterial clearance Increase in bronchial blood vessel permeability
Tissue destruction and secondary inflammatory response results in mucosal slough
Systemic smoke inhalation injury
Decrease in cardiac filling pressure and cardiac index
The inflammatory effects causing capillary leak are complementary following cutaneous burns and inhalation Inflammation within the airways and lung parenchymal injury

3.4 Clinical Setting, Imaging, and Management

A detailed history becomes even more important in such a patient and may help make a difference in the often chaotic setting of the emergency department (ED). Laboratory evaluation and arterial blood gas analysis (particularly the anion, osmolal, and the oxygen saturation gaps) and supportive measures, including the ABCs (airway, breathing, and circulation), may be required (Darling et al. 1996; Mokhlesi and Corbridge 2003; Micak et al. 2007). Unfortunately, the varied presentations result in a nonspecific clinical syndrome (toxidrome) and make diagnosis somewhat difficult (Micak et al. 2007). The Abbreviated Injury Scale (AIS) criteria (0, no injury; 1, mild; 2, moderate; 3, severe; and 4, massive injury) constitute a standardized fiber-optic bronchoscopic (FOB) scoring system for the degree of burn and other inhalational injuries (Endorf and Gamelli 2007; Hassan et al. 2010; Albright et al. 2012; Mosier et al. 2012). Serial tracheobronchial washings for clinical care purposes are usually performed using an antiseptic solution (Miramistin, chlorhexidine gluconate). Blood gas analysis, functional respiratory tests, and FOB results were used to choose an appropriate respiratory support tactics in the patients with inhalation injury.

Despite substantial limitations (Putman et al. 1977), radiography of the chest (CXR) remains the most widely used method for diagnosis and monitoring of many acute inhalational lung diseases. When in admission CXR reveals recent infiltrate, this is evidence of more severe inhalation injury, thereby indicating a worse prognosis (Lee and O'Connell 1988; Wittram and Kenny 1994; DiPoce et al. 2012).

Lung ultrasound (LUS) is an excellent complementary diagnostic tool in emergency diagnosis of tracheal structures, lung consolidation, atelectasis, and pleural effusion; patient safety can be enhanced by performing procedures under US guidance, e.g., thoracentesis and vascular line access (Lichtenstein et al. 2004; Lichtenstein 2014).

Thin-section multidetector computed tomography (MDCT) of the chest is a more sensitive tool to detect inhalation injury, to value its extent, severity, and complications, and continues to demonstrate previously unidentified characteristics that shape our understanding of noxious inhaled toxicant injury (Reske et al. 2005; Koljonen et al. 2007). Since the lung has a fairly uniform response to toxicant injury, the imaging approach to burn and industrial accident victims is similar. Parameters such as estimates of the volume of infusion, as well as assessment of the need for mechanical ventilation management, the possibility of pneumonia development, and outcome are necessary.

The severity of the injury at imaging is directly related to the concentration of the toxicant and the duration of exposure. The choice of imaging studies and the information sought in the patient with a history of inhalation of a toxic gas vary according to the time elapsed since the acute event; we can distinguish:

- The *acute stage or early resuscitation phase* (the first 24–36 h postexposure, as the time the patient is managed in the ED and is usually characterized by acute pulmonary insufficiency); the goal of the radiologist is to document the extent of injury and to determine whether the toxic gas has been inhaled deeply or whether laryngospasm has confined the injury to the upper airway. A *normal CXR*, usually obtained in decubitus AP view at the often unstable patient's bedside at ED admission, may be valuable as a baseline for subsequent CXR or follow-up and does not exclude parenchymal or airway injury *which may only be evident 24–48 h after the acute event* (ARDS latent period), despite clinical evidence of lung injury (arterial hypoxemia, elevated carboxyhemoglobin levels) (Wittram and Kenny 1994). An *abnormal CXR* on admission is variable in severity and extent, indicates a worse prognosis, and may show various disease patterns:
  (a) Subglottic edema with a conical narrowing of the airway, tracheal narrowing, diffuse peribronchial infiltration, moderate venous congestion, peripherally located small round clear bubbles closely arranged to each other in a shape resembling a mulberry, and focal or diffuse patchy opacities that

usually (if not complicated by ARDS) evolve over the first few days or clear within 4–6 days, most likely due to atelectasis and consolidations (Fig. 19). Causes of atelectasis include decreased mucociliary clearance, inspissated secretions of the bronchi and bronchioles, reflex bronchoconstriction, and surfactant inactivation.

(b) Bilateral diffuse alveolar opacities more likely represent progressive noncardiogenic pulmonary edema, by increased permeability diffuse alveolar damage (DAD) with resultant transudation into the alveolar spaces (ARDS), leading to hypoxemia that is refractory to usual oxygen therapy (Ferguson et al. 2012). This can manifest anywhere from mild interstitial edema to pulmonary insufficiency (Fig. 20). ARDS is the final pathway of acute lung injury caused by a variety of agents, including inhaled toxins, aspiration, and infection (George et al. 2003). CXR may help in differentiating it from typical pulmonary edema: CXR features usually develop 12–24 h after initial lung insult, and within 1 week, alveolar pulmonary edema (hyaline membrane) occurs due to type 1 pneumocyte damage.

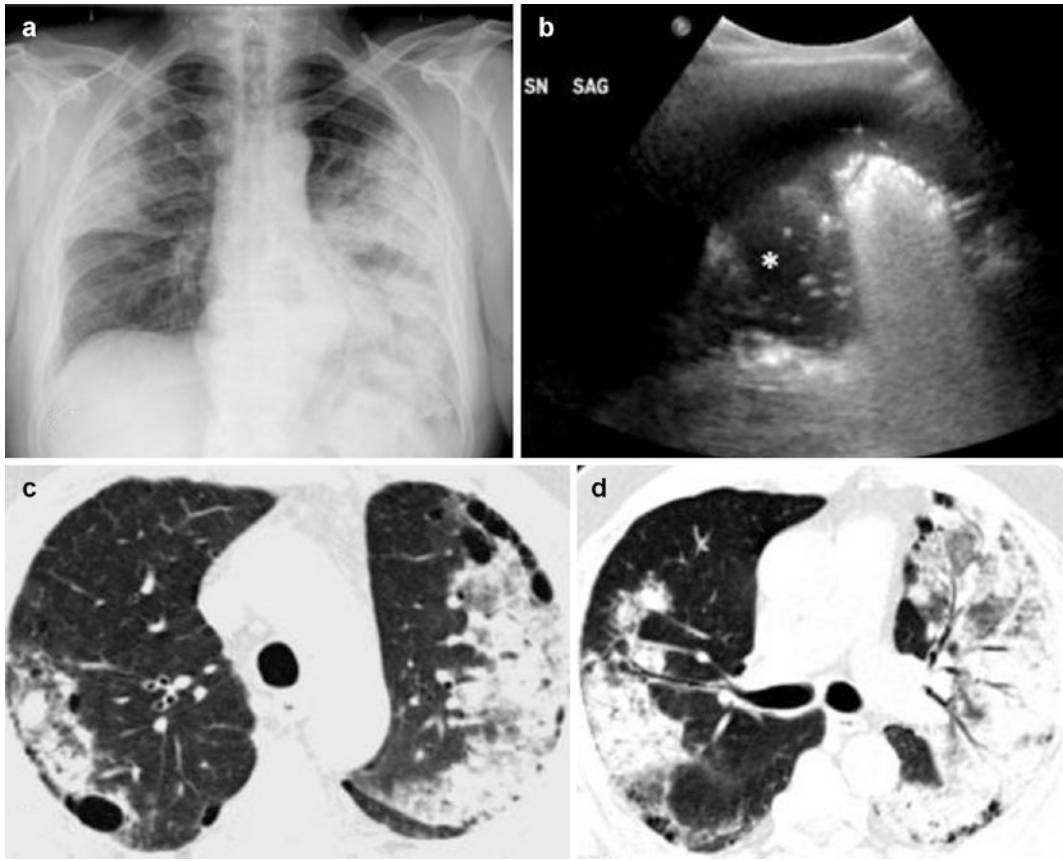

Fig. 19 Integrated imaging (CXR, US, MDCT) of asymmetrical pattern of airspace disease, greater in the left lung, in a 62-year-old man with acute presentation of shortness of breath after 24 h of smoke inhalation (SII). (**a**) CXR on admission shows bilateral consolidations. (**b**) Complementary LUS left sagittal scan shows coexistent pleural effusion and spots (air bronchogram) in consolidated lung (*). (**c**, **d**) MDCT shows airspace consolidation, air bronchograms, and pre-existing subpleural blebs; the bronchial wall thickness (BWT) was 4.2 mm on admission, 4.5 mm after 24 h, and 2.4 mm after 7 days (see text). Bronchoscopic AIS was 3 (severe injury). He developed pneumonia and remained in the ICU for 6 days

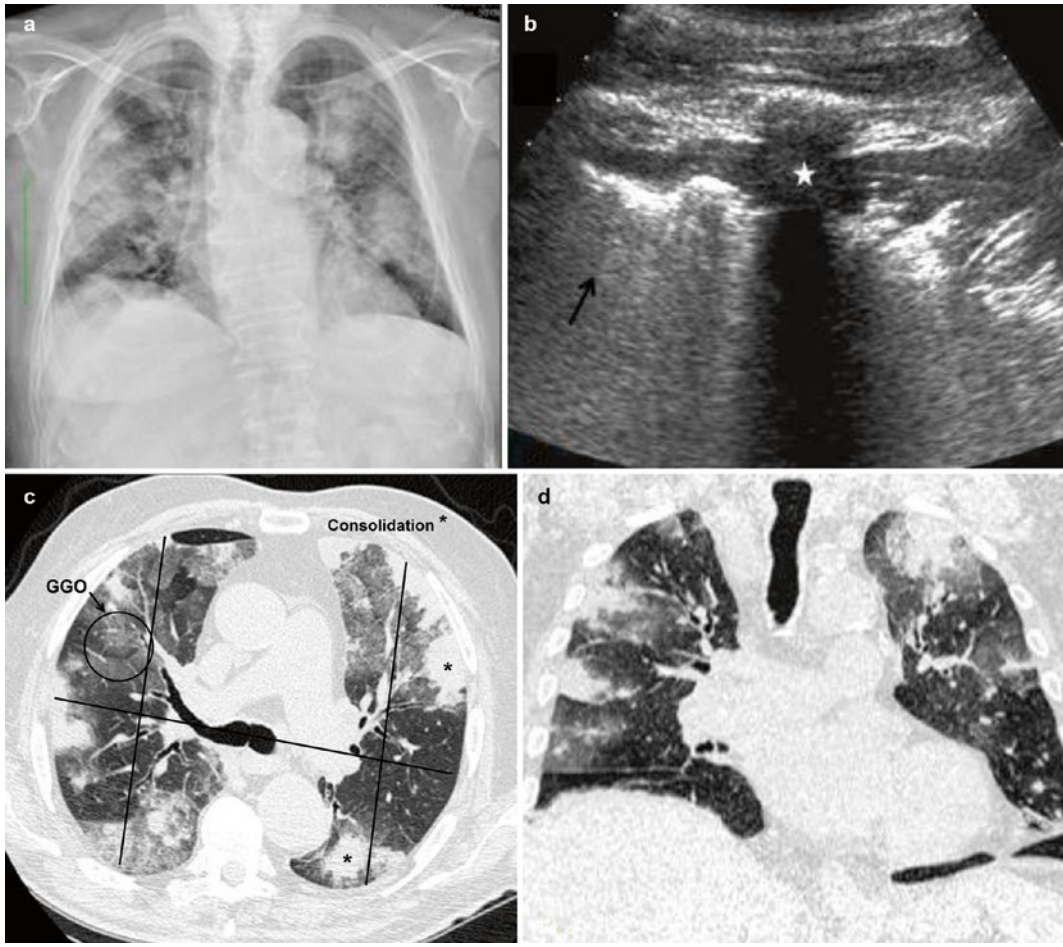

Fig. 20 Integrated imaging (CXR, US, MDCT) in a non-smoking, previously healthy 35-year-old man was presented in the emergency room after an unintentional exposure to chlorine gas at a community swimming pool. (**a**) CXR on presentation shows patchy bilateral lung consolidations. (**b**) Complementary LUS axial scan on the anterior chest at the fifth intercostal space shows focal consolidation (*star*) and aerated lung (*arrow*), without pleural effusion. MDCT (**c**) axial and (**d**) coronal reconstruction scans better demonstrate the extent of focal consolidations (*) and GGO areas; in (**c**) it has shown an example of radiologist's score (RADS) findings in chest CT axial scan (see text)

> In contrast to cardiogenic pulmonary edema, which clears in response to diuretic therapy, ARDS persists for days to weeks. In addition, as the initial radiographic findings of ARDS clear, the underlying lung appears to have a reticular pattern secondary to type 2 pneumocyte proliferation and fibrosis.

In the *acute exudative phase,* pleural effusion, cardiomegaly, and septal lines are typically absent (Gluecker et al. 1999). Injury may progress to mucosal sloughing and intrapulmonary hemorrhage with mechanical obstruction of lower airways, hemoptysis, and flooding of alveoli. Rarely, early alveolar flooding may be caused by retrograde bronchorrhea.

On CXR lung opacities are bilateral, diffuse, patchy, or homogeneous, involving at least three quadrants, and cannot be fully explained by pleural effusion, atelectasis, or nodules (Fig. 21) (Lee and O'Connell 1988; Wittram and Kenny 1994; DiPoce et al. 2012; Fanelli et al. 2013). LUS is superior to auscultation and complementary to bedside CXR in the detection and follow-up of the main lung pathologic entities in ARDS (pleural

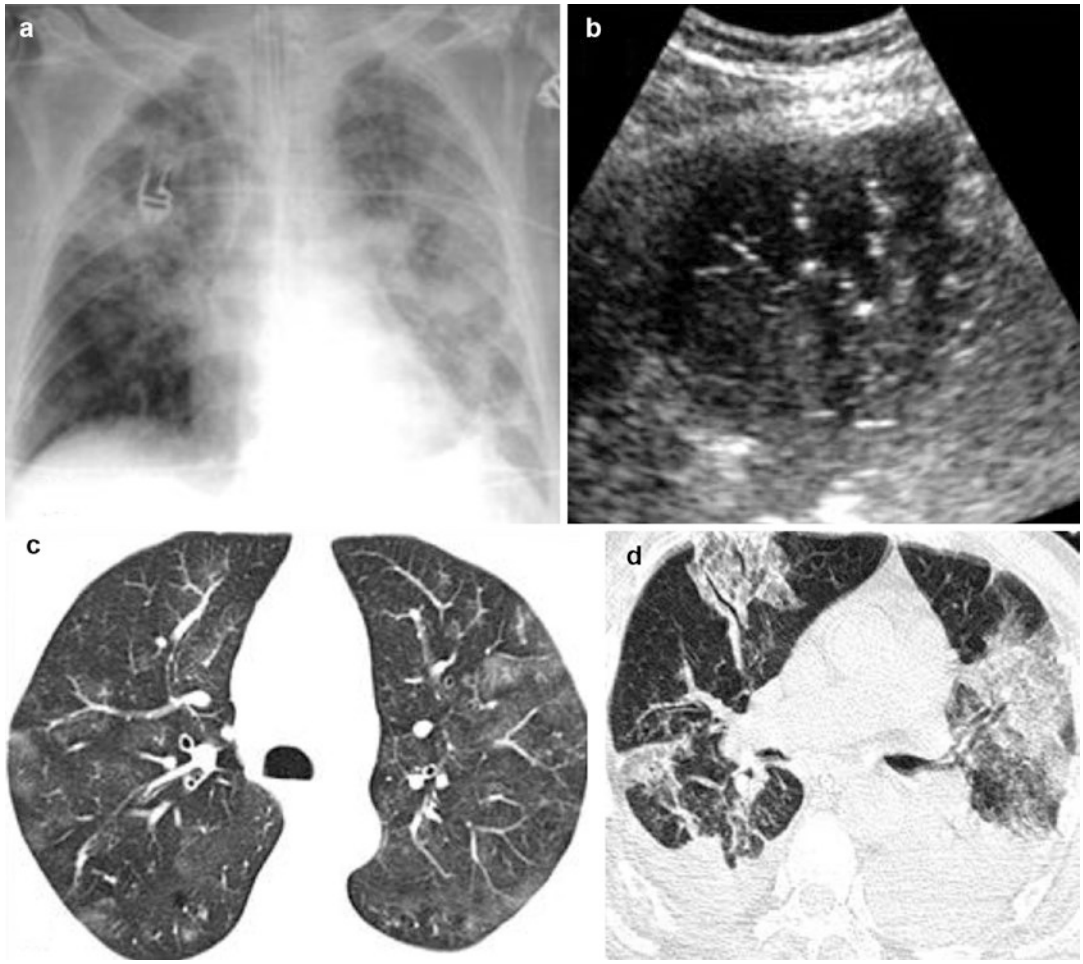

Fig. 21 Integrated imaging (CXR, US, MDCT) in a 43-year-old man working in a chemical industry who was admitted to the emergency department with a complaint of shortness of breath and hemoptysis, which began 3 h after accidental inhalation of nitric acid fumes from falling over the unlocked nitric acid container. He was urgently intubated for respiratory failure approximately 5 h after exposure, and copious serosanguinous secretion was aspirated from endotracheal tube. (**a**) CXR on admission shows bilateral ground-glass opacities. (**b**) Complementary LUS sagittal scan on the lateral chest at the seventh intercostal space shows focal consolidation in the lower left lobe. MDCT (**c**, **d**) axial scans show GGO patchy areas in the upper lobes and widespread GGO with early consolidations in both lower lobes and pleural effusion. Nitric acid is commonly used in various industries and its accidental spillage generates oxides of nitrogen, including nitrogen dioxide, a potent lung toxin when inhaled

effusion, alveolar consolidations, and alveolar-interstitial syndrome), when considering CT as the reference for a correct diagnosis (Lichtenstein et al. 2004; Lichtenstein et al. 2014).

Few hours after injury, MDCT on admission can show subtle ground-glass opacifications with mainly peribronchial distribution and patchy peribronchial consolidations centrally located (Oh et al. 2012; Yamamura et al. 2013) and can be semiquantitatively utilized as a means of stratifying inhalation injury by semiautomated measure of the abnormal lung parenchymal areas: each quadrant of each slice is scored subjectively adding the highest radiologist's score (RADS) (0=normal, 1=interstitial markings, 2=ground-glass appearance, and 3=consolidation) (Park et al. 2003; Oh et al. 2012). A high RADS score (>8 per slice) in addition to a positive bronchoscopy (high AIS score) was associated with a high probability (12.7-fold increase) of pneumonia,

acute lung injury/ARDS, and death, thus showing the potential for chest CT to complement bronchoscopy in detecting clinically significant inhalation injury (Oh et al. 2012). Yamamura et al. used CT imaging to demonstrate the significant association between bronchial wall thickness (BWT) on admission and development of pneumonia; BWT, measured 2 cm distal from the tracheal bifurcation at three time points (at admission, 24 h after, and 7 days after admission), may be a predictor of the severity of SII (Yamamura et al. 2013) (Fig. 22). While the BWT of the normal volunteers is <2 mm, on admission BWT cutoff value of >3.0 mm can predict the total number of ventilator days, ICU stay days, and pneumonia development with a sensitivity of 79 %, specificity of 96 %, positive predictive value of 91 %, and a negative predictive value of 88 % (Yamamura et al. 2013).

In the acute exudative ARDS stage, MDCT shows a gravitationally dependent gradient, with more consolidation in the posterobasal regions, as a result of compressive gravitational forces (Gattinoni and Pesenti 2005). In the acute phase of ARDS, MDCT scans, notwithstanding the difficulties and risks of moving patients from and to the ICU, typically show a nonhomogeneous distribution and a ventrodorsal gradient of density, with more dense consolidations in the dependent regions, widespread ground-glass opacities, and relatively normal or hyperinflated parenchyma (in case of mechanical ventilation) in nondependent areas. Atypical ARDS, characterized by predominantly anterior consolidations in supine decubitus, can be observed in 5 % of patients during the first stage of the disease, probably due to regional differences in ventilation. MDCT predictors of mortality are >80 % of lung involvement, enlargement of the right atrium, or development of traction varicoid bronchiectasis (Chung et al. 2011; Kligerman et al. 2013).

In the *subacute stage or postresuscitation phase* (2–6 days post-injury, characterized by mucosal necrosis and slough, viscous secretions, and distal airway obstruction with atelectasis, pulmonary interstitial edema, and bronchopneumonia), imaging studies are directed toward monitoring

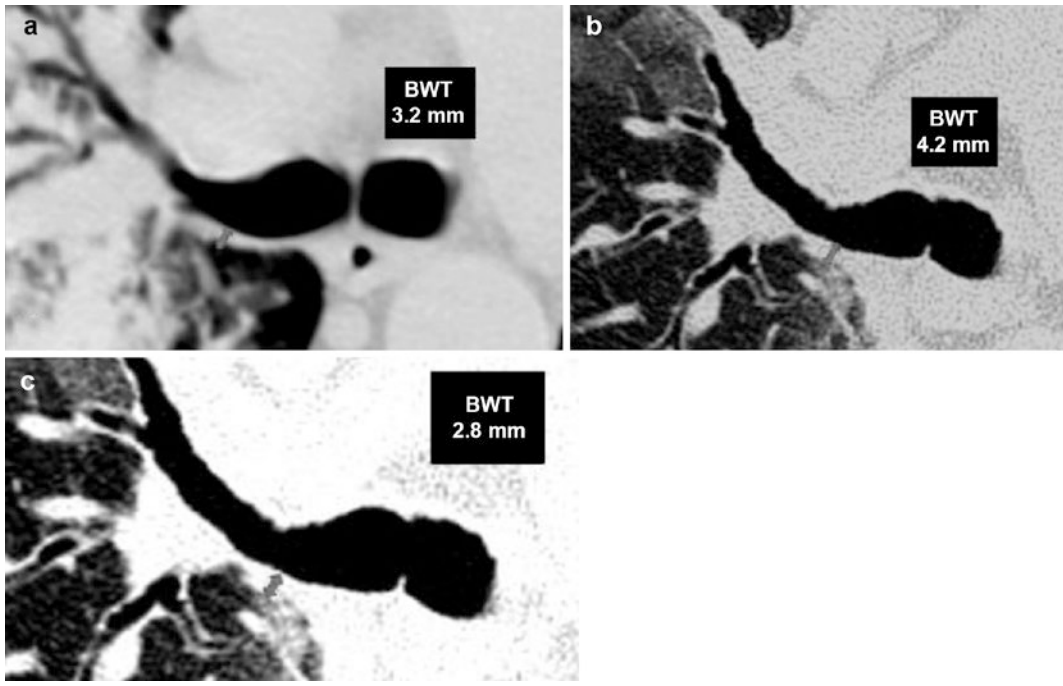

Fig. 22 Indices of bronchial wall thickness (*BWT*) on noncontrast 1 mm helical scan according Yamamura et al. (2013) in a case of smoke inhalation injury (SII). The *double headed arrows* indicate the measurement of bronchial wall thickness (*BWT*) was 3.2 mm on admission (**a**), 4.2 mm after 6 days (**b**), and 2.8 mm after 10 days (**c**). This patient had associated pneumonia and remained in the ICU for 13 days

pulmonary complications in the hospitalized patient (e.g., in burn victims, ranges are from 15 to 42%), including infection, septicemia, ARDS, barotraumas (usually from intubation and positive pressure ventilation), multiorgan failure (MOF), and fluid overload (George et al. 2003). In severely burned patients in ICU, it may be difficult to discriminate among these various components on CXR. The most challenging differential diagnosis is still between ARDS and cardiogenic edema. Because these lung complications are associated with a significant increase in mortality, ranging from 50 to 89%, diagnosis of pulmonary injury is important for both therapeutic and prognostic considerations and must be performed, if it is possible, by thin-slice MDCT. Early signs of barovolutrauma often correspond to interstitial emphysema and subpleural cystic airspaces. Subsequently, imaging studies can demonstrate the development of pneumomediastinum, pneumothorax (often hypertensive in mechanically ventilated patients), and subcutaneous emphysema (Gattinoni et al. 2006) (Fig. 23).

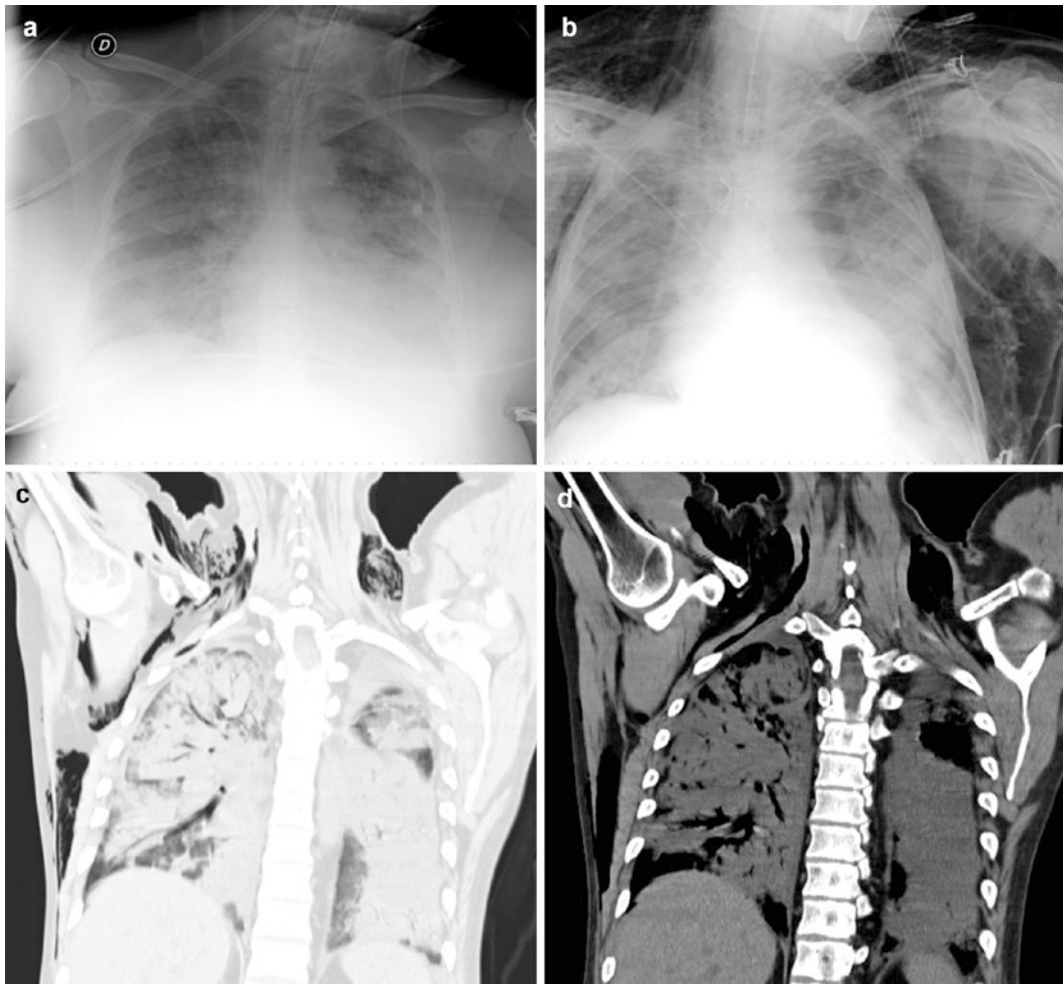

Fig. 23 A 47-year-old male, working at plating industry, was accidentally exposed to HNO3 vapor for 3–4 min. After that accident, he shows mild dyspnea. He suffered from no underlying disease. Ten hours after exposure, ICU admission (**a**) CXR shows diffuse bilateral coalescent GGO opacities in lower lobes. Next day (**b**) follow-up CXR shows extensive pulmonary consolidations appeared at the mid-lower lobes and diffuse subcutaneous emphysema. Four days later, MDCT (**c**, **d**) coronal reconstructions show bilateral progressing consolidations, pleural effusion, and a severe pneumomediastinum with subcutaneous emphysema

Extracorporeal membrane oxygenation (ECMO) is a therapy that has been used in severe cases of ARDS when patients fail to improve with traditional management (Koh 2014).

The *inflammatory–infection phase* and *chronic sequelae of acute exposures* are approximately 7 days and beyond in the post-injury period and continues until there are lung healing and burn wound closure. In intermediate or proliferative phase of ARDS, reticular opacities may appear in the diffuse and persisting background of alveolar opacities; however, unless iatrogenic complications or superimposed pneumonia develops, the radiological findings are rather stable in this phase. The extent of CT opacities (>80 % of lung volume), along with the presence of bronchiectasis, honeycombing, and signs of pulmonary hypertension (dilatation of pulmonary arteries and right ventricle), indicates early fibrosis and predicts mortality (Ichikado et al. 2006). In the later or fibrotic ARDS stage, MDCT generally demonstrates persistent ground-glass densities and reticulations, air cysts, and bullae, mainly located in the ventral regions of the lung, more often than CXR (Masclans et al. 2011). Late exposure complications such as occupational asthma, reactive airway dysfunction syndrome (RADS), increased airway responsiveness, and decreased residual volume have been described. Chronic effects of lower respiratory tract injury include bronchiolitis obliterans, bronchiolitis obliterans organizing pneumonia (BOOP), and pulmonary fibrosis. Bronchiolitis obliterans produces a pattern of fixed airway obstruction that may develop several weeks after injury, following a period in which symptoms improve. Granulation tissue plugs develop within small airways and alveolar ducts, accompanied by small airway destruction with obliterative fibrous scarring.

3.5 Some Unique Pulmonary Acute Toxins and Toxicants

3.5.1 Smoke Inhalation Injury (SII)

"Smoke inhalation" is a generic term that refers to a potential exposure to a wide variety of substances because of the complex chemistry of heat decomposition and pyrolysis (Glazer 2003; Miller and Chang 2003). Thermal airway injury is generally limited to supraglottic structures, whereas injury to the lower airway is chemical in nature. Smoke inhalation injury (SII) complicates burns in approximately 10–20 % of patients and is a major cause of mortality in burn patients because it can trigger pneumonia, acute respiratory distress syndrome (ARDS), and problems with fluid balance (El-Helbawi and Ghareeb 2011; You et al. 2014). Victims of fire accidents may be divided into three categories: those suffering only cutaneous injury, those with cutaneous and inhalational injury, and those with inhalational injury alone (Dries and Endorf 2013). Cutaneous burns are assessed in percent of total body surface area (TBSA) affected by the burn and by evaluating the burn depth. The soot present on the face, in the nose, or in the mouth of a fire victim must raise the suspicion of the inhalation injury. The injury may be limited to the upper airways and manifested by nasopharyngeal irritation, hoarseness, stridor, and dry cough or may extend deeper causing tracheobronchial and alveolar destruction with the symptoms of dyspnea, chest discomfort, bronchial breath sounds, wheezing, rales, cyanosis, and carbonaceous sputum. An abnormal CXR in the first 48 h was stated to be a poor prognostic indicator (Wittram and Kenny 1994; Miller and Chang 2003). The noxious products of combustion induce a laryngotracheobronchitis that may be severe enough to be hemorrhagic, ulcerative, or necrotizing. Surfactant and the surfactant-producing type II pneumocytes may be destroyed or damaged, leading to a DAD, loss of lung compliance, and the damaged vascular endothelium leading to an increased microvascular permeability with resultant edema (Fig. 24).

3.5.2 Paraquat (PQ)

Paraquat is a diquaternary amine aromatic nonselective herbicide whose unintentional or intentional poisoning and mucosal exposure can result in frequently fatal pulmonary toxicity, and this is why it is restricted in some countries. Although it can induce oxygen radical

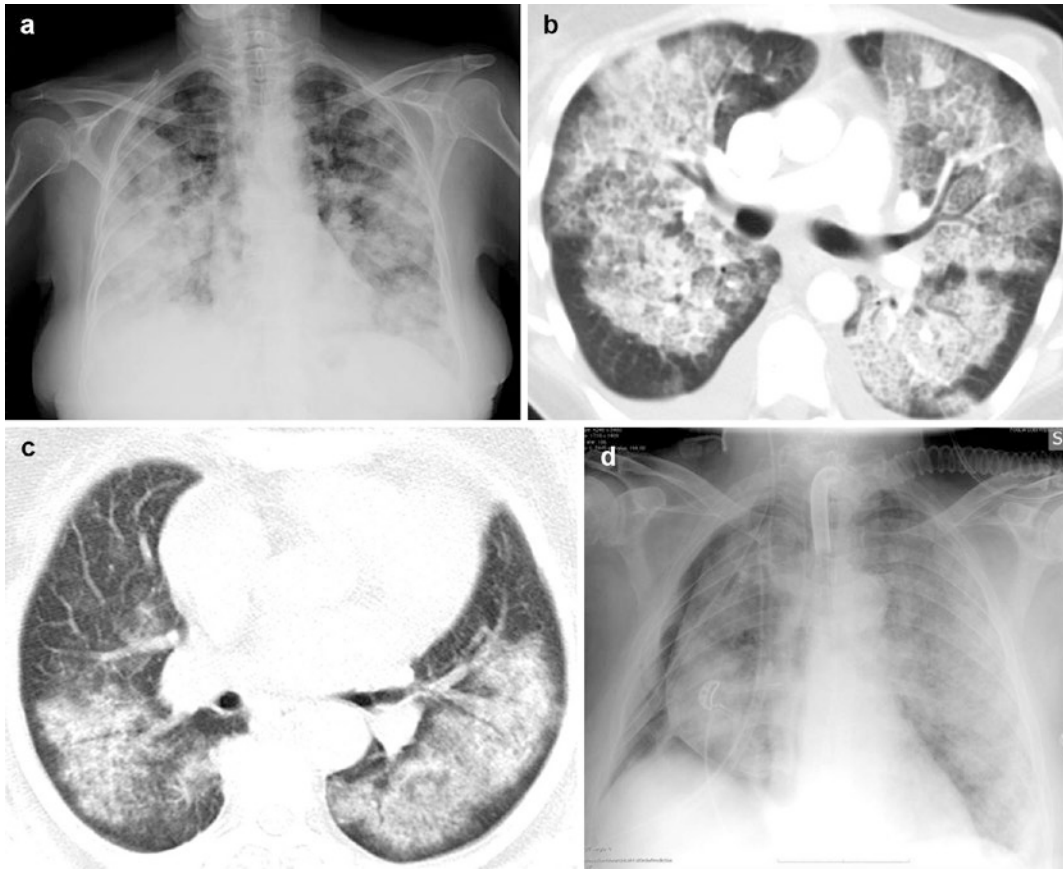

Fig. 24 A 44-year-old man with extensive burns (24 % TBSA) from intentional pouring of petrol, who was then set on fire, with acute presentation and early ICU admission. On the first day, bedside ED (**a**) CXR shows bilateral consolidations. On the fourth day, (**b**, **c**) MDCT axial scans show diffuse bilateral ground-glass opacities sparing the lung periphery and the absence of pleural effusions that are typical of noncardiogenic pulmonary edema. (**d**) Follow-up CXR on the sixth day shows right pneumothorax

formation in all tissues, a structural homology results in its active uptake by pneumocytes from the circulation. The high concentration of polyamine transporters on the luminal side of the type I and type II pneumocytes and club (formerly Clara) cells results in as much as a tenfold concentration of PQ in the pneumocytes (Zhang et al. 2013). Should patients survive the initial caustic ingestion, progressive pulmonary fibrosis with death occurring up to a month later can be expected. In the shortly exposed survivor group, thin-section CT may show ground-glass opacities, consolidations, pleural effusion, and early fibrosis findings (Im et al. 1991; Lee et al. 1995; Kim et al. 2009; Zhang et al. 2013).

3.5.3 Silica

More commonly, chronic inhalation of small amounts of silica (SiO_2), 0.05 mg/m_3, results in predominantly upper lung zone deposition of silica dust that leads to the formation of 1-mm to 10-mm inflammatory nodules and results in local tissue damage. With high-intensity silica acute inhalation, as might be rarely seen in sandblasting or mining, a proliferation of type II pneumocytes can occur, with alveolar proteinosis from excessive surfactant production. This condition is known as acute silicosis also called silicoproteinosis (Dee et al. 1978; Marchiori et al. 2007). Thin-section CT scans show a diffuse GGO (ground-glass opacity) or alveolar pattern with septal thickening, similar

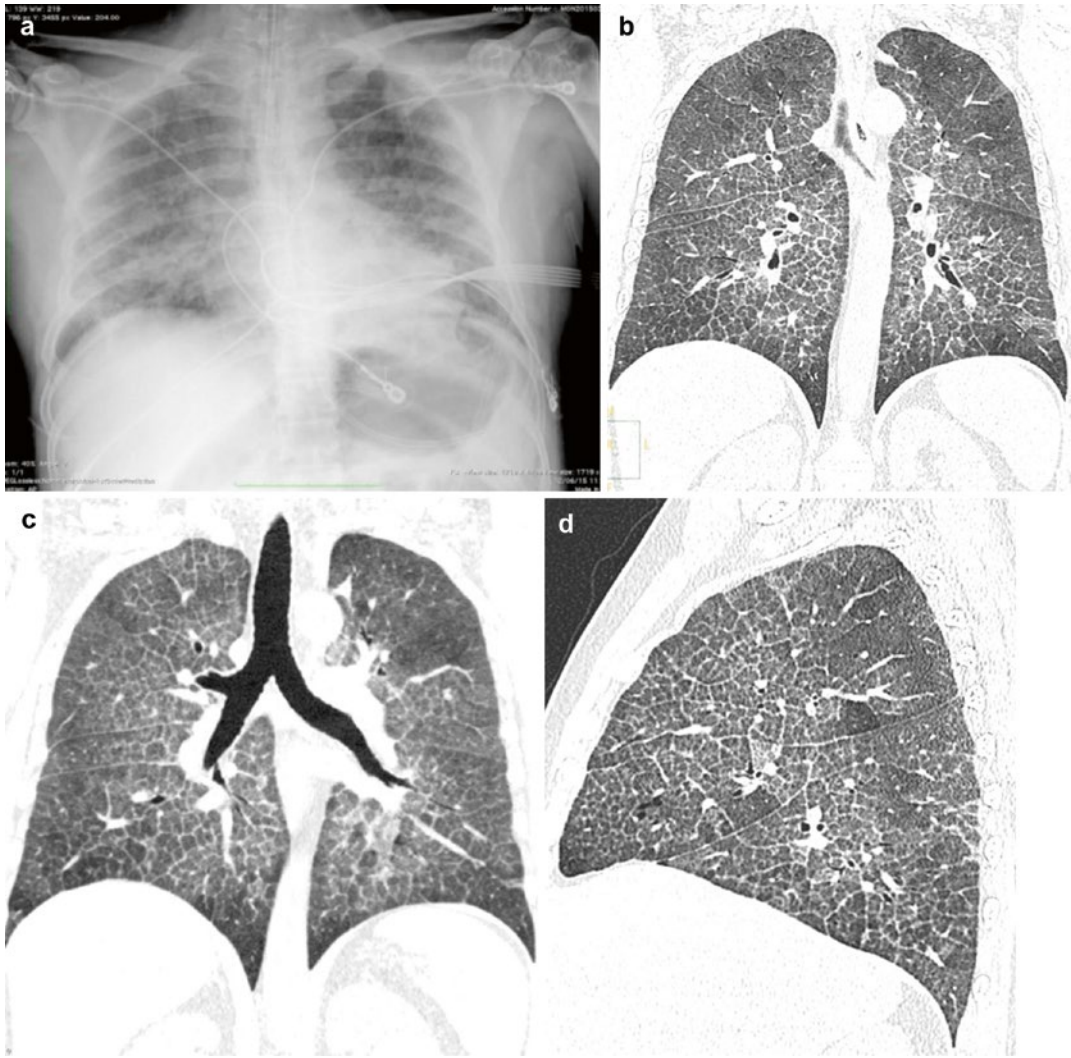

Fig. 25 A rare case of acute silicosis in a 45-year-old-man that was heavily exposed (buried for about 7 h) to very high concentrations of fine silica debris due to the outbreak of his house. He suffered from no underlying disease and had bilateral femoral necks and acetabular comminuted fractures. After about 1 week from the trauma, he presented dyspnea and dry cough. On the sixth day, (**a**) CXR showed diffuse ground-glass appearance of all lung fields. On the eighth day, chest MDCT (**b**, **c**) coronal and (**d**) sagittal reconstructions showed a "crazy-paving" pattern, highly suggestive of secondary alveolar proteinosis

to pulmonary alveolar proteinosis (Buechner and Ansari 1969) (Fig. 25).

3.6 Summary

The lungs can be an efficient means for the absorption of inhaled toxicants, resulting in airway and pulmonary injury or systemic toxicity. Although a few specific antidotes exist for inhaled toxicants, the syndrome of acute inhalation injury and clinical therapeutics are linked by common pathways of pathophysiology. Understanding and prompt diagnosis of the main imaging patterns of acute inhalation injury can simplify the decision-making process for the emergency physicians when confronted with a patient exposed to a myriad of potential inhaled toxicants.

References

Acute exposure guideline levels (AEGLs)|OPPT|US EPA. www.epa.gov/oppt/aegl/

Al Subie H, Fitzgerald DA (2010) Non-cystic fibrosis bronchiectasis. J Paediatr Child Health. doi:10.1111/j.1365-2230.2010.03857.x

Albright JM, Davis CS, Bird MD, Ramirez L, Kim H, Burnham EL et al (2012) The acute pulmonary inflammatory response to the graded severity of smoke inhalation injury. Crit Care Med 40:1113–21. doi:10.1097/CCM.0b013e3182374a67

Aysola RS, Hoffman EA, Gierada D et al (2008) Airway remodeling measured by multidetector computed tomography is increased in severe asthma and correlates with pathology. Chest 134(6):1183–91

Baik JH, Ahn MI, Park YH et al (2010) High-resolution CT findings of re-expansion pulmonary edema. Korean J Radiol 11(2):164–8. doi:10.3348/kjr.2010.11.2.164

Bankier AA, Fleischmann D, Mallek R et al (1996) Bronchial wall thickness: Appropriate window settings for thin-section CT and radiologic-anatomic correlation. Radiology 199:831–6

Bartsch P, Mairbaurl H, Maggiorini M et al (2005) Physiological aspects of high altitude pulmonary edema. J Appl Phys 98:1101–10

Betancourt SL, Martinez-Jimenez S et al (2010) Lipoid pneumonia: spectrum of clinical and radiologic manifestations. AJR Am J Roentgenol 194:103–9

Bhalla M, Turcios N, Aponte V et al (1991) Cystic fibrosis: scoring system with thin-section CT. Radiology 179:783–8

Bonavita J, Naidich PD (2012) Imaging of bronchiectasis. Clin Chest Med 33:233–248

Borron SW, Bebarta VS (2015) Asphyxiants. Emerg Med Clin North Am 33:89–115, http://dx.doi.org/10.1016/j.emc.2014.09.014

Boyton RJ (2012) Bronchiectasis. Medicine. Respir Dis 40(5):267–272

Brander PE, Taskinen E, Stenius-Aarniala B (1992) Fire-eater's lung. Eur Respir J 5:112–114

Brillet PY, Fetita CI, Capderou A et al (2009) Variability of bronchial measurements obtained by sequential CT using two computer-based methods. Eur Radiol 19:1139–47

Brody AS, Sucharew H, Campbell JD et al (2005) Computed tomography correlates with pulmonary exacerbations in children with cystic fibrosis. Am J Respir Crit Care Med 172:1128–1132

Bruzzi JF, Remy-Jardin M, Delhaye D et al (2006) Multidetector row CT of hemoptysis. Radiographics 26:3–22

Buechner HA, Ansari A (1969) Acute silico-proteinosis: a new pathologic variant of acute silicosis in sandblasters, characterized by histologic features resembling alveolar proteinosis. Dis Chest 55:274–278

Bynum LD, Pierce AK (1976) Pulmonary aspiration of gastric contents. Am Rev Respir Dis 114:1129–1136

Causey A, Tilelli J, Swanson M (2000) Predicting discharge in uncomplicated near drowning. Am J Emerg Med 18:9–11

Chang AB, Bilton D (2008) Exacerbations in cystic fibrosis: 4 – non-cystic fibrosis bronchiectasis. Thorax 63:269–76. doi:10.1136/thx.2006.060913

Chung JH, Kradin RL, Greene RE et al (2011) CT predictors of mortality in pathology confirmed ARDS. Eur Radiol 21:730–737

Cole PJ (1984) A new look at the pathogenesis, management of persistent bronchial sepsis: a 'vicious circle' hypothesis and its logical therapeutic connotations. In: Davies RJ (ed) Strategies for the management of chronic bacterial sepsis. Medicine Publishing Foundation, Oxford, pp 1–20

Currie DC, Cooke JC, Morgan AD et al (1987) Interpretation of bronchograms and chest radiographs in patients with chronic sputum production. Thorax 42:278–284

Darling GE, Keresteci MA, Ibanez D et al (1996) Pulmonary complications in inhalation injuries with associated cutaneous burn. J Trauma 40:83–89

Davies G, Wells AU, Doffman S, Watanabe S, Wilson R (2006) The effect of Pseudomonas aeruginosa on pulmonary function in patients with bronchiectasis. Eur Respir J 28:974–9

de Jong PA, Ottink MD, Robben SGF et al (2004) Pulmonary disease assessment in cystic fibrosis: comparison of CT scoring systems and value of bronchial and arterial dimension measurements. Radiology 231:434–439

Dee P, Suratt P, Winn W (1978) The radiographic findings in acute silicosis. Radiology 126:359–63

DiPoce J, Guelfguat M, DiPoce J (2012) Radiologic findings in cases of attempted suicide and other self-injurious behavior. Radiographics 32:2005–2024

Dodd JD, Souza CA, Muller NL (2006) Conventional high-resolution CT versus helical high-resolution MDCT in the detection of bronchiectasis. AJR Am J Roentgenol 187:414–420

Dries DJ, Endorf FW (2013) Inhalation injury: epidemiology, pathology, treatment strategies. Scand J Trauma Resusc Emerg Med 21:31

Du Rand I, Maskell N, Hooper C, Lee YCG et al (2010) British Thoracic Society Pleural Disease Guideline Group: a sub-group of the British Thoracic Society Standards of Care Committee. Management of spontaneous pneumothorax. Thorax 65(Suppl 2):ii18–eii31. doi:10.1136/thx.2010.136986

Echevarria C, Twomey D, Dunning J et al (2008) Does re-expansion pulmonary oedema exist? Interact Cardiovasc Thorac Surg 7:485–9

El-Helbawi RH, Ghareeb FM (2011) Inhalation injury as a prognostic factor for mortality in burn patients. Ann Burns Fire Disasters XXIV(2):82–88

Endorf FW, Gamelli RL (2007) Inhalation injury, pulmonary perturbations, and fluid resuscitation. J Burn Care Res 28:80–83

Fagenholz PJ, Gutman JA, Murray AF et al (2007) Chest ultrasonography for the diagnosis and monitoring of high-altitude pulmonary edema. Chest 131:1013–8

Fanelli V, Vlachou A, Ghannadian S et al (2013) Acute respiratory distress syndrome. New definition, current and future therapeutic options. J Thorac Dis 5:326–334

Feldman C (2011) Bronchiectasis: new approaches to diagnosis and management. Clin Chest Med 32:535–546. doi:10.1016/j.ccm.2011.05.002

Ferguson ND, Fan E, Camporota L et al (2012) The Berlin definition of ARDS: an expanded rationale, justification, and supplementary material. Intensive Care Med 38:1537–1582

Franquet T, Gimenez A, Roson N et al (2000) Aspiration diseases: findings, pitfalls, and differential diagnosis. Radiographics 20:673–85

Fujimoto K, Kitaguchi Y, Kubo K et al (2006) Clinical analysis of chronic obstructive pulmonary disease phenotypes classified using high-resolution computed tomography. Respirology 11:731–40

Garnier R (1998) Acute toxic pneumopathies. Rev Prat 48:1319–23

Gattinoni L, Pesenti A (2005) The concept of "baby lung". Intensive Care Med 31:776–784

Gattinoni L, Caironi P, Valenza F et al (2006) The role of CT-scan studies for the diagnosis and therapy of acute respiratory distress syndrome. Clin Chest Med 27:559–570

George A, Gupta R, Bang RL, Ebrahim MK (2003) Radiological manifestation of pulmonary complications in deceased intensive care burn patients. Burns 29:73–78

Glazer CS (2003) Acute inhalational injury. In: Hanley ME, Welsh CH (eds) Current diagnosis & treatment in pulmonary medicine, Internationalth edn. Mc-Graw Hill, New York, pp 354–60

Gluecker T, Capasso P, Schnyder P et al (1999) Clinical and radiologic features of pulmonary edema. Radiographics 19(6):1507–31

Goeminne P, Dupont L (2010) Non-cystic fibrosis bronchiectasis: diagnosis and management in 21st century. Postgrad Med J 86:493–501

Gorguner M, Aslan S, Inandi T, Cakir Z (2004) Reactive airways dysfunction syndrome in housewives due to a bleach-hydrochloric acid mixture. Inhal Toxicol 16:87–91

Gotway MB, Lee ES, Reddy GP et al (2000) Low-dose, dynamic, expiratory thin-section CT of the lungs using a spiral CT scanner. J Thorac Imaging 15:168–72

Grenier P, Maurice F, Musset D et al (1986) Bronchiectasis: assessment by thin-section CT. Radiology 161:95–99

Gudbjerg CE (1955) Roentgenologic diagnosis of bronchiectasis. An analysis of 112 cases. Acta Radiol 43:209–217

Guimaraes MD, Bitencourt AGV, Marchiori E, Chojniak R, Gross JL, Kundra V (2014) Imaging acute complications in cancer patients: what should be evaluated in the emergency setting? Cancer Imaging 14:18

Hansell DM (1998) Bronchiectasis. Radiol Clin North Am 36:107–28

Hansell DM, Bankier AA, MacMahon H, McLoud TC, Müller NL, Remy J (2008) Fleischner Society: glossary of terms for thoracic imaging. Radiology 246:697–722. doi:10.1148/radiol.2462070712

Hassan Z, Wong JK, Bush J, Bayat A, Dunn KW (2010) Assessing the severity of inhalation injuries in adults. Burns 36:212–6. doi:10.1016/j.burns.2009.06.205

Heitkamp DE, Mohammed TL, Kirsch J et al (2012) ACR appropriateness criteria (®)acute respiratory illness in immunocompromised patients. J Am Coll Radiol 9:164–9

Hill LE, Ritchie G, Wightman AJ, Hill AT, Murchison JT (2010) Comparison between conventional interrupted high-resolution CT and volume multidetector CT acquisition in the assessment of bronchiectasis. Br J Radiol 83:67–70

Houston CS (1960) Acute pulmonary edema of high altitude. N Engl J Med 263:478–80

Hunter TB, Whitehouse WM (1974) Fresh-water near-drowning: radiological aspects. Radiology 112:51–56

Ichikado K, Suga M, Muranaka H et al (2006) Prediction of prognosis for acute respiratory distress syndrome with thin section CT: validation in 44 cases. Radiology 238:321–329

Idris AH, Berg RA, Bierens J et al (2003) Recommended guidelines for uniform reporting of data from drowning: the "Utstein style". Circulation 108:2565–74

Im JG, Lee KS, Han MC, Kim SJ, Kim IO (1991) Paraquat poisoning: findings on chest radiography and CT in 42 patients. AJR Am J Roentgenol 157:697–701. doi:10.2214/ajr.157.4.1892020

Javidan-Nejad C, Bhalla S (2009) Bronchiectasis. Radiol Clin North Am 47:289–306. doi:10.1016/j.rcl.2008.11.006

Javidan-Nejad C, Bhalla S (2010) Bronchiectasis. Thorac Surg Clin 20:85–102

Kales SN, Christiani DC (2004) Acute chemical emergencies. N Engl J Med 350:800–8

Kim JS, Muller NL, Park CS et al (1997a) Bronchoarterial ratio on thin section CT: comparison between high altitude and sea level. J Comput Assist Tomogr 21:306–311

Kim JS, Muller NL, Park CS et al (1997b) Cylindrical bronchiectasis: diagnostic findings on thin-section CT. AJR Am J Roentgenol 168:751–754

Kim YT, Jou SS, Lee HS, Gil HW, Yang JO, Lee EY et al (2009) The area of ground glass opacities of the lungs as a predictive factor in acute paraquat intoxication. J Korean Med Sci 24:636–40. doi:10.3346/jkms.2009.24.4.636

King PT, Daviskas E (2010) Pathogenesis and diagnosis of bronchiectasis. Breathe 6:343–51

Kligerman S, Franks T, Galvin J (2013) Organization and fibrosis as a response to lung injury in diffuse alveolar damage, organizing pneumonia, and acute fibrinous and organizing pneumonia. Radiographics 33:1951–1975

Koh Y (2014) Update in acute respiratory distress syndrome. J Intensive Care 2:2. doi:10.1186/2052-0492-2-2. http://www.jintensivecare.com/content/2/1/2

Koljonen V, Maisniemi K, Virtanen K, Koivikko M (2007) Multi-detector computed tomography demonstrates smoke inhalation injury at early stage. Emerg Radiol 14:113–6

Kosucu P, Ahmetoglu A, Koramaz J et al (2004) Low-dose MDCT and virtual bronchoscopy in pediatric

patients with foreign body aspiration. AJR Am J Roentgenol 183:1771–1777
Laurent F, Philippe JC, Vergier B et al (1999) Exogenous lipoid pneumonia: HRCT, MR, and pathologic findings. Eur Radiol 9:1190–96
Lee MJ, O'Connell DJ (1988) The plain chest radiograph after acute smoke inhalation. Clin Radiol 39:33–37
Lee SH, Lee KS, Ahn JM, Kim SH, Hong SY (1995) Paraquat poisoning of the lung: thin-section CT findings. Radiology 195:271–4
Lichtenstein D, Goldstein D, Mourgeon E et al (2004) Comparative diagnostic performances of auscultation, chest radiography, and lung ultrasonography in acute respiratory distress syndrome. Anesthesiology 100:9–15
Lichtenstein D (2014) Lung ultrasound in the critically ill. Curr Opin Crit Care 20:315–22
Lichtenstein D, van Hooland S, Elbers P, Malbrain ML (2014) Ten good reasons to practice ultrasound in critical care. Anaesthesiol Intensive Ther 46:323–35. doi: 10.5603/AIT.2014.0056
Lynch DA (1998) Imaging of asthma and allergic bronchopulmonary mycosis. Radiol Clin North Am 36(1):129–42
Marchiori E, Souza CA, Barbassa TG et al (2007) Silicoproteinosis: high-resolution CT findings in 13 patients. AJR Am J Roentgenol 189:1402–6
Martinez S, Heyneman LE, McAdams HP, Rossi SE, Restrepo CS, Eraso A (2008) Mucoid impactions: finger-in-glove sign and other CT and radiographic features. Radiographics 28:1369–82
Masclans JR, Roca O, Munoz X et al (2011) Quality of life, pulmonary function, and tomographic scan abnormalities after ARDS. Chest 139:1340–1346
McCollough CH, Primak AN, Braun N, Kofler J, Yu L, Christner J (2009) Strategies for reducing radiation dose in CT. Radiol Clin North Am 47:27–40
McCurdy MT, Shanholtz CB (2012) Oncologic emergencies. Crit Care Med 40:2212–2222
McKay CA Jr (2014) Toxin-induced respiratory distress. Emerg Med Clin North Am 32:127–147, http://dx.doi.org/10.1016/j.emc.2013.09.003
Micak RP, Suman OE, Herndon DN (2007) Respiratory management of inhalation injury. Burns 33:2–13
Miller K, Chang A (2003) Acute inhalation injury. Emerg Med Clin North Am 21:533–557
Milliron B, Henry TS, Veeraraghavan S, Little BP (2015) Bronchiectasis: mechanisms and imaging clues of associated common and uncommon diseases. Radiographics 35:1011–30. doi:10.1148/rg.2015140214
Mokhlesi B, Corbridge T (2003) Toxicology in the critically ill patient. Clin Chest Med 24:689–711
Montella S, Santamaria F, Salvatore M et al (2009) Assessment of chest high-field magnetic resonance imaging in children and young adults with noncystic fibrosis chronic lung disease: comparison to high resolution computed tomography and correlation with pulmonary function. Invest Radiol 44:532–8
Mosier MJ, Pham TN, Park DR, Simmons J, Klein MB, Gibran NS (2012) Predictive value of bronchoscopy in assessing the severity of inhalation injury. J Burn Care Res 33:65–73
Naidich DP, McCauley DI, Khouri NF et al (1982) Computed tomography of bronchiectasis. J Comput Assist Tomogr 6:437–444
Nelson LS, Hoffman RS (2006) Inhaled toxins. In: Marx JA, Hockberger RS, Walls RM (eds) Rosen's emergency medicine: concepts and clinical practice, 6th edn. Mosby Elsevier, Philadelphia
Oh JS, Chung KK, Allen A, Batchinsky AI, Huzar T, King BT et al (2012) Admission chest CT complements fiberoptic bronchoscopy in prediction of adverse outcomes in thermally injured patients. J Burn Care Res 33:532–8. doi:10.1097/BCR.0b013e318237455f
Oikonomou A, Tsanakas J, Hatziagorou E et al (2008) High resolution computed tomography of the chest in cystic fibrosis (CF): is simplification of scoring systems feasible? Eur Radiol 18:538–547
Ooi GC, Khong PL, Chan-Yeung M et al (2002) High-resolution CT quantification of bronchiectasis: clinical and functional correlation. Radiology 225:663–72
Pappalettera M, Aliberti S, Castellotti P et al (2009) Bronchiectasis: an update. Clin Respir J 3:1752–6981
Park MS, Cancio LC, Batchinsky AI, McCarthy MJ, Jordan BS, Brinkley WW et al (2003) Assessment of severity of ovine smoke inhalation injury by analysis of computed tomographic scans. J Trauma 55:417–27. doi:10.1097/01.TA.0000083609.24440.7F
Patel IS, Vlahos I, Wilkinson TM et al (2004) Bronchiectasis, exacerbation indices, and inflammation in chronic obstructive pulmonary disease. Am J Respir Crit Care Med 170:400–7
Pratali L, Cavana M, Sicari R et al (2010) Frequent subclinical high-altitude pulmonary edema detected by chest sonography as ultrasound lung comets in recreational climbers. Crit Care Med 38:1818–23
Putman CE, Loke J, Matthay RA, Ravin CE (1977) Radiographic manifestations of acute smoke inhalation. AJR Am J Roentgenol 129:865–70. doi:10.2214/ajr.129.5.865
Quint LE (2009) Thoracic complications and emergencies in oncologic patients. Cancer Imaging 9:S75–S82
Rabe KF, Hurd S, Anzueto A et al (2007) Global strategy for the diagnosis, management, and prevention of chronic obstructive pulmonary disease: GOLD executive summary. Am J Respir Crit Care Med 176: 532–55
Rabinowitz PM, Siegel MD (2002) Acute inhalation injury. Clin Chest Med 23:707–715
Reid LM (1950) Reduction in bronchial subdivision in bronchiectasis. Thorax 5:233–47
Reske A, Bak Z, Samuelsson A, Morales O, Seiwerts M, Sjöberg F (2005) Computed tomography – a possible aid in the diagnosis of smoke inhalation injury? Acta Anaesthesiol Scand 49:257–60
Rossi SE, Franquet T, Volpacchio M et al (2005) Tree-in-bud pattern at thin-section CT of the lungs: radiologic-pathologic overview. Radiographics 25:789–801
Salem H, Katz SA (eds) (2015) Inhalation toxicology, 3rd edn. CRC Press/Taylor & Francis group, Boca Raton
Shoemark A, Ozerovitch L, Wilson R (2007) Aetiology in adult patients with bronchiectasis. Respir Med 191:1163–70

Siafakas NM, Anthonisen NR, Georgopoulos D (eds) (2004) Management of acute exacerbation of COPD. Marcel Dekker Inc., New York

Studler U, Gluecker T, Bongartz G, Roth J, Steinbrich W (2005) Image quality from high-resolution CT of the lung: comparison of axial scans and of sections reconstructed from volumetric data acquired using MDCT. AJR Am J Roentgenol 185:602–7

Sung YM, Lee KS, Yi CA, Yoon YC, Kim TS, Kim S (2003) Additional coronal images using low-milliamperage multidetector-row computed tomography: effectiveness in the diagnosis of bronchiectasis. J Comput Assist Tomogr 27:490–5

Swenson ER, Maggiorini M, Mongovin S et al (2002) Pathogenesis of high-altitude pulmonary edema: inflammation is not an etiologic factor. JAMA 287(17):2228–35

Szpilman D, Bierens JJLM, Handley AJ, Orlowski JP. (2012) Drowning. N Engl J Med 366:2012–10

Tan CK, Lai CC (2007) Neurogenic pulmonary edema. CMAJ 177(3):249–50

Tourigny PD, Hall C (2012) Diagnosis and management of environmental thoracic emergencies. Emerg Med Clin North Am 30:501–528. doi:10.1016/j.emc.2011.10.006

Westcott JL (1991) Bronchiectasis. Radiol Clin North Am 29:1031–42

Williamson JP, James AL, Phillips MJ et al (2009) Quantifying tracheobronchial tree dimensions: methods, limitations and emerging techniques. Eur Respir J 34:42–55

Wittram C, Kenny JB (1994) The admission chest radiograph after acute inhalation injury and burns. Br J Radiol 67:751–4

Woodring JH (1994) Improved plain film criteria for the diagnosis of bronchiectasis. J Ky Med Assoc 92:8–13

Woods AQ, Lynch DA (2009) Asthma: an imaging update. Radiol Clin North Am 47:317–329. doi:10.1016/j.rcl.2008.11.008

World Health Organization. Causes of death 2008 summary tables. Available at: http://www.who.int/evidence/bod. Accessed 14 June 2011

Yadav SP, Singh J, Aggarwall N et al (2007) Airway foreign bodies in children: experience of 132 cases. Singapore Med J 48:850–853

Yamamura H, Kaga S, Kaneda K et al (2013) Chest computed tomography performed on admission helps predict the severity of smoke-inhalation injury. Crit Care 17:R95. doi:10.1186/cc12740

You K, Yang HT, Kym D, Yoon J, Haejun Y, Cho YS et al (2014) Inhalation injury in burn patients: establishing the link between diagnosis and prognosis. Burns 40:1470–5. doi:10.1016/j.burns.2014.09.015

Young K, Aspestrand F, Kolbenstvedt A (1991) High resolution CT and bronchography in the assessment of bronchiectasis. Acta Radiol 32:439–41

Zhang H, Liu P, Qiao P, Zhou J, Zhao Y, Xing X, Li G (2013) CT imaging as a prognostic indicator for patients with pulmonary injury from acute paraquat poisoning. Br J Radiol 86(1026):20130035. doi:10.1259/bjr.20130035

Zissin R, Shapiro-Feinberg M, Rozenman J et al (2001) CT findings in the chest in adults with aspirated foreign bodies. Eur Radiol 11:606–611